IEEE Access
Multidisciplinary ⋮ Rapid Review ⋮ Open Access Journal

Received 11 September 2023, accepted 26 October 2023, date of publication 30 October 2023,
date of current version 15 November 2023.

Digital Object Identifier 10.1109/ACCESS.2023.3328582

RESEARCH ARTICLE

Tool Health Classification in Metallic Milling Process Using Acoustic Emission and Long Short-Term Memory Networks: A Deep Learning Approach

FAWAD KHAN[1], KHURRAM KAMAL[1], TAHIR ABDUL HUSSAIN RATLAMWALA[1], MOHAMMED ALKAHTANI[2], MOHAMMED ALMATANI[2], AND SENTHAN MATHAVAN[3], (Member, IEEE)

[1]Department of Engineering Sciences, National University of Sciences and Technology, Islamabad 44000, Pakistan
[2]Department of Industrial Engineering, College of Engineering, King Saud University, Riyadh 11421, Saudi Arabia
[3]Department of Civil and Structural Engineering, Nottingham Trent University, NG1 4BU Nottingham, U.K.

Corresponding author: Fawad Khan (fawadkhan630@gmail.com)

This work was supported by King Saud University, Riyadh, Saudi Arabia, through the Researchers Supporting Project under Grant RSP2023R274.

ABSTRACT The manufacturing industry has experienced remarkable progress as a result of integrating automated and intelligent production processes fueled by technological innovation, leading to substantial advancements. These advanced processes involve the use of flexible and high-performance machines, tackling complex and sophisticated processing problems with ease. However, the processing performance can deteriorate due to tool damage or malfunction, which can lead to the discarding of workpieces. Hence, it carries immense importance to have a close look over the condition of the tool throughout the processing to proactively address any potential issues and minimize the possibility of significant tool failures, particularly when manufacturing intricate and costly machine components. Many researchers have looked at the use of machine learning and deep learning approaches for monitoring tool condition. In this study, we are incorporating time series sequential data for which LSTM is the best opted technique. It further explains, how deep learning using Long Short-Term Memory Networks (LSTM) and the acoustic data acquired through a microphone during the metallic milling process has a potential and achieved impressive results. In our study, the accuracy of the model was assessed for different workpiece materials, including Aluminum, Mild Steel, and Brass, and demonstrated the model's ability to make highly accurate predictions. Specifically, the model achieved an average test accuracy of 99.03% for Aluminum workpieces, while achieving very good test accuracies of 97.16% and 97.83% for Mild Steel and Brass workpieces, respectively. These results were benchmarked against previous work in the same domain, confirming the efficacy of the model.

INDEX TERMS Long short-term memory networks (LSTM), model test accuracy, tool condition monitoring.

I. INTRODUCTION

Development of a tool health detection and classification system has got significant importance in modernization of manufacturing industry. As a conventional procedure, tool wear monitoring and classification was performed by human operators who used to visually inspect the tool and make decisions based on their expertise. However, this is a subjective approach with high probability of error, ultimately leading to unnecessary tool replacements or even

The associate editor coordinating the review of this manuscript and approving it for publication was Zijian Zhang.

machining failures. With the advent of new technological developments like artificial intelligence (AI), said procedures have been revolutionized and so as the tool health monitoring process. Traditional, AI systems use rule-based models to analyze sensor data and determine the tool's health condition. These systems require the selection of relevant features and pre-processing of sensor data, which not only are time-consuming but require significant domain knowledge as well. However, advanced AI techniques, such as machine learning (ML), have shown great potential in improving the accuracy and efficiency of tool health classification. ML models learn from data patterns without the explicit need for complex and sophisticated programming, making them more adaptable to changing conditions and capable of handling intricate data. By directly extracting characteristics from the unprocessed data obtained through data acquisition systems, deep learning (DL) has also demonstrated promise in the categorization of tool wear. The development of a tool health classification system using advanced AI techniques helps improve tool wear detection accuracy, reduction in machine downtime, increase productivity, and reduce maintenance costs. Moreover, it can provide real-time monitoring, providing ease in decision-making, which ultimately lead to improved overall machining efficiency.

II. LITERATURE REVIEW

A. ACOUSTIC EMISSION AND TOOL HEALTH MONITORING

CNC based turning operation using a lathe machine was conducted in Industrial Automation Lab of College of E&ME NUST, Islamabad and AE sensor was used for data acquisition. The experiment utilized Denford Cyclone-P CNC turning machine. The Learning Vector Quantization (LVQ) algorithm was employed which successfully classified the tool states into three categories, and the predictions were validated using the trained network [1]. Researchers at the Industrial Automation Lab in NUST, Islamabad Pakistan implemented a procedure to collect data from airborne acoustic signals during milling processes on soft and hard wood. The study involved three conditions of tools including new, used, and worn-out for both types of wood and separate backpropagation neural networks were trained for softwood and hardwood. The average accuracy for classification of tool condition was 97% for hardwood and 78.4% for softwood [2]. A study focused on tool health monitoring using acoustic emission signals (AE Signals) and a Convolutional Neural Network (CNN) approach was executed in Industrial Automation Lab of the College of E&ME, NUST Islamabad. The raw signals were transformed into 2D images, fed and trained as input to CNN architecture and evaluated using algorithm validation. The proposed technique achieved a consistent accuracy of over 99% for all cases, showcasing the effectiveness of acoustic emission and deep learning-based health monitoring using CNN [3]. Scientists conducted research to develop tool wear system by analyzing acoustic emission signals in a drilling process on mild-steel workpiece. Using Chebyshev-1 band pass filter, the acoustic signals were filtered out and analyzed in the time and time-frequency domains to extract drilling process-sensitive features. Artificial neural network is trained by adopting the back-propagation learning algorithm. The proposed ANN model exhibited satisfactory performance and could be implemented in automated drilling processes for tool wear monitoring [4]. A PSO-optimized back-propagation neural network based novel approach is proposed for monitoring CNC turning tool health, leveraging airborne acoustic emission signals. The method involves capturing acoustic signals using a microphone for tools in different conditions, the RMS values of the depth of cut signal and spindle RPM. The model training and optimization is performed using a PSO algorithm for classifying tool health. Said neural network outperforms the simple back-propagation network, and achieved an enhanced accuracy valued as 68.94% compared to 49.24%. [5].

B. CUTTING FORCE AND TOOL HEALTH MONITORING

A tool breakage detection system accompanied by self-learning for CNC end-milling operations, utilizing a Probabilistic Neural Network is proposed. The data collected during experimentation was trained and analyzed using a PNN toolbox in MATLAB Simulink. The system aimed to achieve high accuracy through gradual parameter adjustments and addressed errors by activating the self-learning mechanism [6]. A sensor-less approach for detecting tool fractures in milling processes, focused on observer-based cutting force and torque estimation. The model was validated through multiple milling tests on an aluminum alloy. The results demonstrated high estimation accuracy in identifying small fluctuations in cutting force. The study highlighted the effectiveness of this sensor-less approach, offering potential improvements in efficiency and reliability in real-time tool fracture detection [7]. In peripheral milling of particleboard, tool dulling is studied using a tungsten carbide tool. The researchers discovered the relation of varied tool wear over the cutting edge due to differences in workpiece thickness density. The study provides valuable insights into tool wear accompanied by dulling characteristics in peripheral milling of particleboard [8].

C. CURRENT SIGNALS AND TOOL HEALTH MONITORING

An approach utilized adaptive synthetic sampling to predict the tools' remaining usable life. It employed a bidirectional long-short term memory (LSTM) network for analysis, avoiding manual feature extraction. Spindle motor drive current signals are collected through a sensor, and the signal with the highest correlation is chosen for subsequent analysis using a DC method. The experimental setup involved a machining center, current converter, and sensor for data acquisition, with varied cutting parameters. The bidirectional LSTM technique accurately predicted the remaining useful life of the tool without requiring manual feature extraction [9]. An LSTM-based model is used for envisaging

tool wear in the flank during high-speed turning processes. Experiments were performed on a Nexus 100-II M CNC machine using a steel bar as the workpiece and a carbide tool. The current clamp (CP6550-NA), LabVIEW software, and MATLAB were used for signal acquisition, monitoring, and analysis, respectively. Right at the entrance and exit during cutting, features were extracted from the raw signals. The dataset has been divided into sets of training, testing and validation with 67%, 8% and 25% respectively [10]. The authors presented an application of discrete wavelet transformation to monitor end mill cutter failure using spindle motor current. The experiment involved using an HSS helical end mill cutter and measuring the spindle current with a C/V sensor. The Haar wavelet method was applied over the detected current signals and were processed and decomposed. This process indicated tool failure by detecting changes [11].

D. VIBRATION ANALYSIS AND TOOL HEALTH MONITORING

Condition based maintenance was followed using vibration signal analytics which resulted in enhanced accuracy and quality. This technique enabled detection of faults and potential issues at very initial stages, preventing machine breakdowns and production downtime. The study concluded that condition-based maintenance accompanied by vibration analysis is a productive tool when working on high-value machines and components [12]. A hardware signal processing unit (HSP), during machining process, captured and digitalized the vibration signals. It was part of a reconfigurable system for high-speed milling operations for both online and real-time tool condition monitoring. The signal was decoded in a reconfigurable IIR bandpass digital filter and applied to an entire field of programmed gates and ROMs. The experimental setup comprised a numerically controlled 3-axis DM 4326 vertical machine and an aluminum alloy 6061-T6 workpiece. The results of this study showed that the entire reconfigurable system was able to detect and identify tool condition with 100% accuracy [13]. The aim of the research was to predict the surface roughness in machining methods using least square support vector machine (LS-SVM) based roughness prediction model and valuable information was obtained by singular spectrum analysis (SSA) decomposition. The LS-SVM estimation method was found to be suitable for accurate surface roughness predictions [14]. A study presents a fault diagnosis method for tool faults in numerical control machines by incorporating stationary subspace analysis (SSA) and LS-SVM using a single sensor. SSA extracts both stationary as well as non-stationary sources from multi-dimensional signals, which then trains the LS-SVM using ten statistical indexes. The proposed SSA + LS-SVM method surpassed 80% accuracy figure for tool fault diagnosis, outperforming other methods [15]. The study focused on tool condition monitoring in milling using the actual signal as well as the demodulated one for measurements of vibration during the cutting process. The signals were recorded using a sensor and digitized using an analog-to-digital converter. The researchers found that spindle vibration monitoring through an accelerometer was the most effective approach. If an unacceptable condition was detected, the operator would be alerted to take appropriate action [16]. Researchers demonstrated the use of vibration analysis to detect and track damage to an end mill during milling. The vibration signals were analyzed using various processing schemes alongside scalogram and mean frequency variation. The results showed that scalogram and mean frequency were effective in identifying restricted and advanced faults, even in the presence of noise. The global average of mean frequency variation was found to be a useful indicator of wear progression [17].

E. FEATURES ANALYSIS AND TOOL HEALTH MONITORING

A comparative study over milling process for the detection of tool wear by employing spindle motor load and eddy current sensors was performed. This activity was performed on a Denford CNC type milling machine with aluminum workpiece. The eddy current sensors IC12-02, two of its kind, are mounted in a biaxial manner connected to PDA 3502A type power supply. MATLAB accompanied by automated signal and sensor processing selection approach is used for extraction of sensitive features [18]. The main parameters and factors used in an indirect and online monitoring system for machining process are acoustic emission, microphone, vibration and spindle sensor data. It was concluded from our simulation that the nonparametric charts performed best for our scenarios and the standard charts performed well for the microphone data but performed poor for the triaxial accelerometer data [19]. A TCMS for turning was presented, utilizing acoustic and feed motor current signals. LS-SVM estimated the feed current, while SSA was applied to the cutting criteria as input to the TCMS [20]. For turning process, a new tool condition monitoring solution was presented, utilizing extended subtractive clustering and adaptive neural fuzzy inference system. Experimental results showed lower RMS value and higher prediction errors compared to other artificial intelligence techniques using the same dataset [21]. A neural network-based sensor fusion model for tool health monitoring has been developed and validated in laboratory and industrial environments. The back-propagation learning model was trained and validated through multiple milling operations using a tungsten carbide tool and various machining parameters [22]. In a paper, it was suggested to analyze both the cutting force and the vibration signals on the basis of frequency and time-frequency to determine how much longer the high-speed micro-milling process would be helpful. The experimental design comprised cutting tests performed NCT VHTC-130M micro-milling machine. A total of 15 experiments were conducted by varying feed rate, cutting speed, depth of cut and its direction of cut, their cutting signals were acquired, processed and analyzed using both the techniques of frequency and time-frequency analysis [23].

TABLE 1. Model benchmarking.

S. #	Reference	Approach	Application	Avg. Accuracy
1.	M. Arsalan et al. [3]	"Convolutional Neural Network (CNN)"	Tool Life Prediction - Teflon, MS and Al workpieces	98.4%
2.	Madhusudana [28]	"K-Star Algorithm"	Fault Diagnosis - Face Milling	96%
3.	R. H. L. Da Silva et al. [29]	"Probabilistic Neural Network (PNN)"	Tool Life Prediction - AE and Cutting Power Signals	91%
4.	S. Rangwala and D. Dornfeld [30]	"Artificial Neural Network (ANN)"	Tool health prediction using noisy signals	95%
5.	Yu et al. [31]	"Hidden Markov Model (HMM)"	Tool health classification and life conjecture	81.64%
6.	T. Zafar [5]	"PSO-Optimized Neural Network"	Tool health monitoring in turning process	68.94%
7.	T. Zafar [2]	"Back-Propagation Neural Network"	Wood Milling Process	87.7%
8.	Proposed Technique	"Long Short-Term Memory (LSTM)"	Tool health classification of end mill cutter	**98.01%**

A setup for tool wear condition monitoring was designed using common current sensors over servo-motor of a CNC turning center for estimation of cutting force. Surprisingly, this system showed an accuracy up to 95% of feed cutting force [24]. A comprehensive review of TCM methods in milling processes was conducted, focusing on sensors, feature extraction, and monitoring models which concluded with suggestions for future research in the field [25]. The study investigated the use of Neural Network models to classify power system states to as whether it is secure or not. The Pattern Recognition (PR) approach was employed, involving pre-processing, feature extraction, and classification. Several neural network models, including Learning Vector Quantization, Multilayer Perceptron, Adaptive Resonance Theory Mapping (ARTM) and Probabilistic Neural Network were tested for static and transient security evaluation. Performance evaluation metrics such as mean squared error (MSE), classification accuracy (CA), and misclassification rate (MC) were used. The models were applied to standard IEEE test systems of different sizes and compared in terms of their training and testing performance [26]. The research is aimed with objective to detect tool wear in the drilling process by analyzing sound and vibration signals. Statistical features were extracted from signals' time and frequency-based spectrums and Wavelet Packet Decomposition (WPD) was applied. The study assessed the effectiveness of acoustic and vibration signals in detecting drill wear and concluded that WPD offered improved differentiation compared to primary time domain signals [27]

F. MODEL BENCHMARKING

Considerable work is performed in the field of tool health classification using different AI based algorithms. Different algos offer varying applications with reference to problem in question. In tool health classification domain, our proposed model has been benchmarked against the previous work performed. The details of proposed work-up is explained in detail in the upcoming sections of this paper. However, the proposed model showed an average accuracy of 98.01% and has been benchmarked against different work previously been executed as shown in table 1 above.

III. PROPOSED TECHNIQUE

Multiple AI based techniques have been implemented for tool health classification of different machining processes. One of the important ones is using recurrent neural network (RNN) for time series patterns of data. However, in our case of acoustic data, one of the challenges encountered by RNNs will be the occurrence of two problems: exploding gradients and vanishing gradients which are caused by the size of the gradient. Too small gradient continues to diminish during updates of the weight parameters till they become trivial and equals zero. The problem of vanishing gradient is addressed by LSTMs using a set of gated memory cells that are specifically designed to preserve information over long term dependencies in time series sequential data. These memory cells use a combination of input, forget, and output gates that retain or discard information at each time step, thus allows and learn the network to maintain important information over long time periods. The three key reasons of using LSTM for time series sequential data are:

A. The long-term dependency which allows it to remember historical data significantly impacting our future predictions.

B. Our data comprises variable time-series, which can be easily handled by the LSTM model

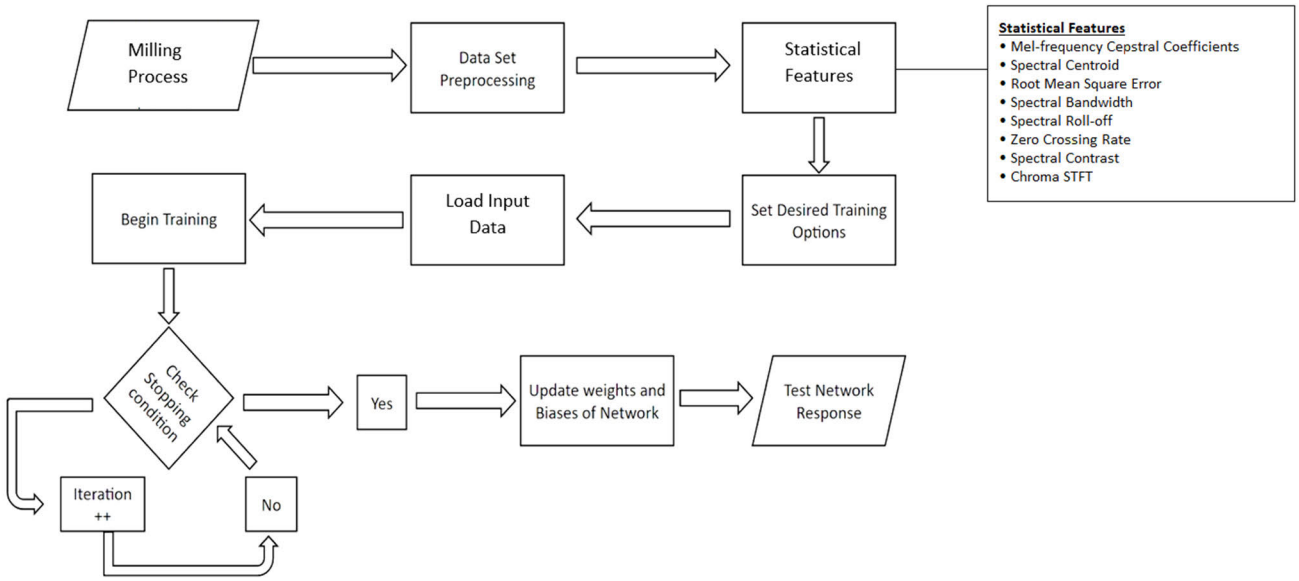

FIGURE 1. Process flow chart.

C. The property of features extraction and handling multivariate sequential data.

The proposed technique is shown in flow chart in figure 1 above.

A. LONG SHORT-TERM MEMORY NETWORKS (LSTM)

Recurrent Neural Networks (RNNs) use a backpropagation with time algorithm to compute gradients, which differs slightly from traditional backpropagation because it is adapted to serial data. Back propagation through time (BPTT) enables the model to train itself by calculating errors from the output layer to the input layer, allowing for appropriate parameter adjustments and fitting. However, BPTT differs from traditional approach as it involves stepwise summation of errors, whereas feedforward networks do not require error summation as their parameters are not shared across layers.

One of the challenges that RNNs face is the existence of two problems, which are exploding gradients and vanishing gradients. These problems generate from the size of gradient, which represents the slope of the loss function on the error curve. When the gradient is too small, it will decrease while updating the weight parameters until they become trivial and equal to 0. Consequently, the algorithm cannot learn. On the other hand, too large gradient refers to exploding gradients, leading to an unstable model. This problem can cause the model weights to increase significantly.

To address these issues, one potential solution is incorporating decreasing number of hidden layers in the neural network, thereby reducing some of the complexities in the RNN model and a typical LSTM model is adapted from [32] implicated in figure 2 below:

B. WORKING OF LSTM NETWORKS

LSTM has a chain like structure but the repeating layers has a different as additional four interacting layers (σ, σ, Tanh, σ,)

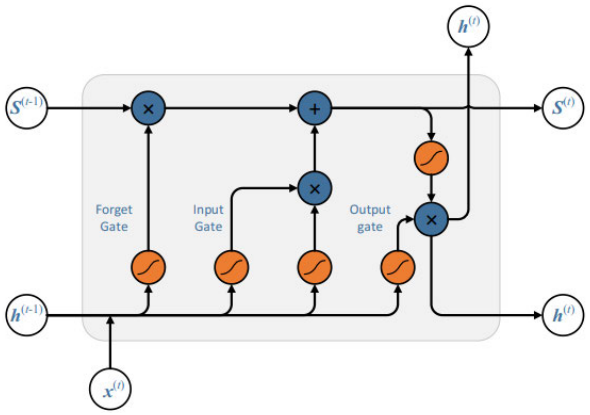

FIGURE 2. Typical LSTM model.

are interacting during the learning procedure. Typical working of LSTM Networks works in three steps as follows.

1) FORGET GATE

LSTM's first phase is decision over information to be kept in the cell and which to discard, based on the present input and previous hidden state. This is done through a series of gates, including the forget gate which uses a sigmoid activation function to determine which information should be discarded.

The forget gate takes the last hidden state (h_t-1) and the present input (x_t), concatenates them, and feeds them into a sigmoid activation function. The output of sigmoid function ranges from zero to one and represents the degree to which each element of the previous hidden state should be forgotten. A zero value means that the element should be completely forgotten, while value of 1 show that the element should be completely retained. An equation of forget gate is shown

TABLE 2. Milling machine details.

S. No.	Machine	Details
1.	Machine	PAK OERLEKON Conventional Milling
2.	Type	LK4 U00 (Vertical type)
3.	Model	1986
4.	Serial	K4 00238
5.	Manufacturer	Pakistan Machine Tool Factory (PMTF)

in equation 1.

$$f_t = \sigma\left(W_f\left[h_{t-1}, x_t\right] + b_f\right) \tag{1}$$

where, $\mathbf{f_t}$ denotes the forget gate.

2) INPUT GATE

The input gate, on other hand, consists of two parts: Tanh function and a sigmoid function. The sigmoid function is used to decide which information from the earlier hidden and contemporary input state should be updated, while the hyperbola of tangent function helps in creating a new candidate cell state that will be added to the updated cell state.

The output value of sigmoid function is between zero and one, representing the degree to which each element of the last hidden and present input should be updated. A value of 0 means that the element should be completely ignored, while 1 means that the element should be completely updated. The gate may be mathematically represented as in equation 2:

$$i_t = \sigma\left(w_i\left[h_{t-1}x_t\right] + b_i\right) \tag{2}$$

$$\tilde{c}_t = \tanh\left(w_c\left[h_{t-1}, x_t\right] + b_c\right). \tag{3}$$

where, i_t represents the input gate.

3) OUTPUT GATE

For obtaining our output, the output gate serves the purpose. A sigmoid function is run which shows the layers making it to the output layer. The cell state is set by applying hyperbolic of Tangent for pushing the value somewhere in between -1 and 1 which is multiplied to the output of sigmoid layer. Mathematically, output gate is illustrated as follows in equation 4 and equation 5:

$$O_t = \sigma\left(W_0\left[h_{t-1}x_t\right] + b_0\right) \tag{4}$$

$$h_t = O_t \times \tanh\left(C_t\right) \tag{5}$$

where, $\mathbf{O_t}$ represents the output gate.

IV. EXPERIMENTAL PROCEDURE AND SETUP

The complete experimental process for proposed study was performed at Engineering Workshop of Pakistan Security Printing Corporation (PSPC), Karachi. The complete experimentation setup was made over milling machine and all instances of experiment were recorded over it. Details of Machine are tabulated as follows:

During the complete experimental procedure, the revolution per minute (RPM) of machine spindle and feed rate f of workpiece for machining were kept unchanged at 450 rpm and 0.5 mm/sec respectively. The depth of cut (DOC) was our variable for different cases of experiment starting from 1mm ...4mm. Three types of workpieces were used for our experiment: Mild Steel (MS), Brass and Aluminum. High speed steel (HSS) cutting tool having fixed diameter of 10 mm was used. Three conditions of tools i.e.: New, Used and Worn-out tools were used for recording the data. Further details of aforementioned is elucidated as follows:

A. CUTTING TOOLS

The end mill cutter used during the experimentation is made of HSS (High Speed Steel) having diameter of 10 mm. High speed steel (HSS) cutters are commonly used in machining and cutting operations due to their ability to withstand high temperatures and maintain their hardness at elevated temperatures. HSS cutters are well known for their hardness, toughness and wear resistance and therefore used over most metals and alloys. As per our analytical requirements, we used said tool in three states which are new, used and worn-out. New tool is never used before, used one is used to a limited extent with its cutting edges worn-out slightly while the worn-out tool has dents and cuts ingested in its cutting edges and used severely. Metallic Workpieces

Three metallic workpieces were used for our experiment.

A. Mild Steel

B. Brass

C. Aluminum

Mild steel is a type of carbon steel that contains a low amount of carbon, typically around 0.05-0.25%. Mild steel is one of the most commonly used materials in construction and manufacturing industries due to its affordability, strength, and versatility. It is a ferrous material as contains iron and an alloy as well, containing other elements in addition to iron and carbon, such as manganese, sulfur, and phosphorus.

Copper and Zinc combines to make Brass with both metals in varying proportions based on desired properties. Traces of other elements such as Lead, Manganese, and Iron can also be added to further modify its properties. Brass bears yellowish-gold color with excellent malleability and good

corrosion-resistant properties, making it a prevalent choice for decorative applications.

FIGURE 3. Three types of tools (Front and top view).

Aluminum is popular for its lightweight, silver-white color with excellent strength-to-weight ratio, low density and resistant to corrosion. Aluminum is a highly versatile metal and used extensively in multiple applications including construction, transportation, packaging and electronics. It is often alloyed with other metals, such as Copper, Magnesium, and Zinc, to improve its properties. The three states of cutters used are shown in figure 3; the three workpieces and a microphone used in experimentation process are shown in figure 4 as follows:

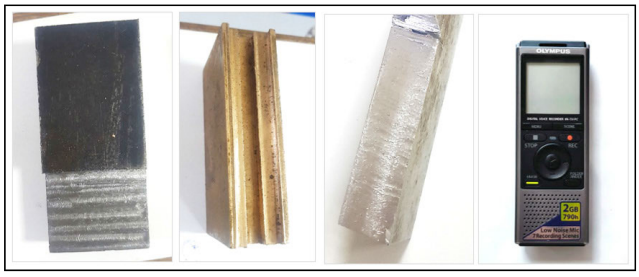

FIGURE 4. Three types of Workpieces & Microphone.

B. ACOUSTIC SIGNAL ACQUISITION AND ANALYSIS

Acoustic signal acquisition is acquiring acoustic signals and converting them into electrical signals for further processing by a computer or other electronic device. The process involves the use of a microphone or other relevant transducer to convert the sound waves into an electrical pulse that can be amplified and further processed. Several factors have impact over acoustic signals acquisition process, such as the type of microphone or transducer being used, position of the microphone with respect to the sound source, and the ambient noise level in the environment. Once the acoustic signal is acquired and converted to electrical pulse, it can be processed using techniques like filtering, amplification, and digital signal processing (DSP). The processed signal is ready to be used for diverse range of applications, including speech recognition, audio recording, noise cancellation, or acoustic imaging.

Tool health classification is performed using the acoustic data of machining process generated due to contact of tool and workpiece. In experimentation step, multiple instances of audio sound signals are acquired through a simple microphone placed in closed vicinity of 5mm. End milling is performed over the aforementioned three types of workpieces with 1mm incremental depth of cut starting from 1mm and using all the three conditions of tools i.e.: new used and worn-out. Accordingly, acoustic data is captured and transferred to a local hard drive. A typical digital voice recorder, OLYMPUS VN-731 PC was used during the experimentation that is shown in figure below. This voice recorder operates in the audible frequency range of 20Hz to 20kHz having sampling frequency of 44.1kHz.

The acoustic data acquired during the experimentation step was analyzed using Google Colaboratory (Colab) allowing users writing and running options for Python code in a Jupyter Notebook environment.

C. FEATURES OF ACOUSTIC DATA

Extracting meaningful features from acoustic data is an essential step in machine learning applications involving audio analysis. Features extraction from acoustic data involves selecting relevant characteristics of the signal that uses to represent the signal in a ML model. The choice of feature extraction method depends on the specific application and the type of audio data being analyzed.

Our aim is to use long short-term memory network (LSTM) as training model for our acoustic data acquired during milling process. The selection of features for an LSTM model should consider their relevance to the task, discriminative power, robustness to noise and variability, efficiency and scalability. By considering these criteria, the selected features can help the LSTM model learn the underlying patterns in the data and improve its performance. The features selected are incorporated in analytical procedures through different libraries already imported in active directory of Google Colab. Aforementioned said, the features selected for our analysis include:

Mel-frequency Cepstral Coefficients (MFCCs)
Spectral Centroid
Root Mean Square Error (RMSE)
Spectral Bandwidth
Spectral Roll-off
Zero Crossing Rate (ZCR)
Spectral Contrast
Chroma STFT

1) MEL-FREQUENCY CEPSTRAL COEFFICIENTS (MFCCS)

Mel Frequency Cepstral Coefficients (MFCCs) are a set of features that are commonly used in audio processing

applications and based for machine learning algorithm representing the spectral characteristics of a signal.

The MFCCs are derived by first applying a series of signal processing techniques, including framing, windowing, and the Fourier Transform, to convert the audio waveform into a time-frequency representation. The Mel scale is then used to convert the domain of frequency axis to Mel scale. The logarithm of the power spectrum is taken and the Discrete Cosine Transform (DCT) is executed over the resulting spectrum. The first few coefficients obtained from the DCT represent the low-frequency components of the spectrum, while the later coefficients capture the higher-frequency components. The conversion factors to and from Mel scale are stated below in equation 6 and equation 7:

Frequency to Mel Scale:

$$M(f) = 1125 \ln(1 + f/700) \tag{6}$$

Mel Scale to frequency:

$$M^{-1}(m) = 700\left(exp\left(\frac{m}{1125}\right) - 1\right) \tag{7}$$

The resulting MFCCs conveys a compact and informative representation of the spectral characteristics of an audio signal.

2) SPECTRAL CENTROID

Spectral centroid is a feature typically used in audio signal processing and information retrieval tasks. The spectral centroid shows the ''center of mass'' of the power spectral density (PSD) of an audio signal and represents the point of energy concentration at a specific frequency.

Mathematically, the spectral centroid represents the weighted average of the frequency values, where the weights are given by the power spectral density as in equation 8:

$$SC = \frac{\sum_{i=1}^{n} iP(f_i)}{\sum_{i=1}^{n} P(f_i)} \tag{8}$$

SC represents the spectral centroid, where n is number of frequency bins in the PSD, f_i is the frequency and P (f_i) shows the power spectral density at i. In speech recognition tasks, SC can be used to identify different natures of acoustics through their characteristic styles. Spectral centroid is an explicit feature that gives valuable insights into the spectral content of an audio signal in a diverse range of machine learning applications.

3) ROOT MEAN SQUARE ERROR (RMSE)

Root Mean Square Error (RMSE) is a metric used in machine learning for assessing performance of regression models. It measures the difference between the actual and the predicted values and mathematically, can be represented as in equation 9:

$$\text{RMSE} = \sqrt{\frac{\sum_{i=1}^{n} (y_{pred} - y_{actual})^2}{N}} \tag{9}$$

where n denotes the number of samples in the dataset, y_{pred} and y_{actual} are the predicted and actual values respectively.

The RMSE value ranges from 0 to infinity, the lower indicating better model performance. A value of 0 confirms matching of the predicted and actual values, while larger values indicate larger errors in model predictions.

4) SPECTRAL BANDWIDTH

Spectral bandwidth shows the range of frequencies present in a spectrum and may be calculated as the difference between the maximum and the lowermost frequency components in a spectrum. In acoustic processing, spectral bandwidth measures the range of frequencies present in the spectral envelope of a signal. It is useful for characterizing the spectral properties and been used as a feature in machine learning models for speech recognition tasks. Spectral bandwidth is calculated the Fourier Transform (FT), Short-Time FT or Wavelet Transform, depending on the nature of the signal under analysis.

5) SPECTRAL ROLL-OFF

Spectral roll-off feature is used in machine learning for audio signal processing tasks such as speech recognition and audio fingerprinting. It deals with the amount of spectral energy below a certain frequency threshold and is defined as the frequency under which a percentage of the total spectral energy exists. Spectral roll-off is a feature to represent the spectral shape of an audio signal and by extracting this feature and using it as input to a machine learning model, the model can learn to classify the audio signal based on its spectral shape. This can be useful for applications in vast domain, such as, speech recognition, and audio content-based retrieval.

6) ZERO CROSSING RATE

Features like zero crossing rate are generally used in machine learning for audial signal processing like speech recognition, music genre classification, and audio fingerprinting. The zero-crossing rate explains the number of times an audio signal shift between positive and negative value within a given time frame. It is used as a feature to represent the progressive design of an audio signal in domain of machine learning. The chronological shape of an audio signal provides information about the characteristics of the sound source like the rhythm, tempo, or pitch. Zero-crossing rate features when fed as input to an ML model can learn to classify the audio signal based on its temporal structure.

7) SPECTRAL CONTRAST

The difference between neighboring frequency bands' spectral energies is measured via spectral contrast. An audio signal's spectral structure is represented by it as a feature. Audio signal's spectral structure can provide details about the timbre, tone, or harmonic content of the sound source. A machine learning model may learn to identify an audio signal based on its spectral structure by extracting the spectral contrast feature from it and feeding it as input to it. Spectral

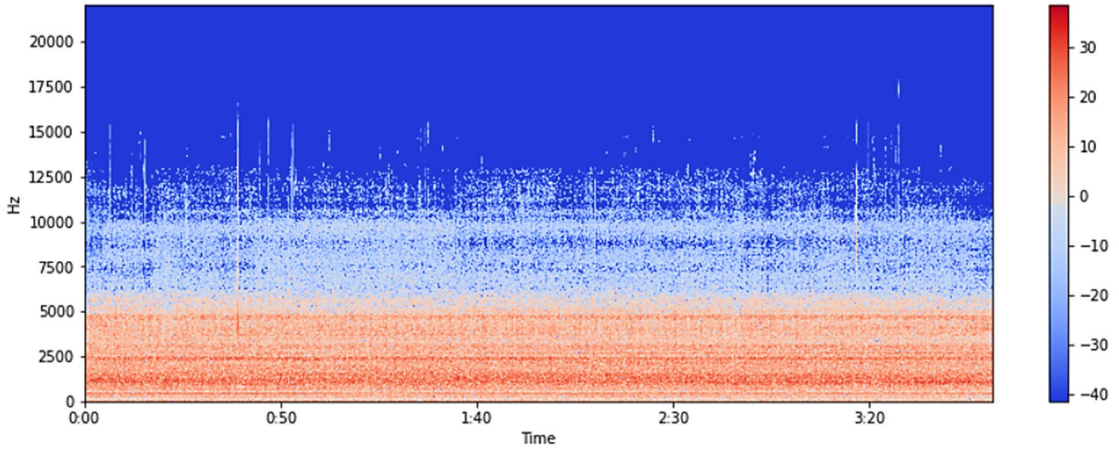

FIGURE 5. Spectrogram of aluminum.

contrast can offer more details about the spectral makeup of an audio stream and improve machine learning performance.

8) CHROMA STFT

Chroma STFT is a characteristic used in machine learning for applications like music genre categorization, chord identification, and audio fingerprinting that require audio signal processing. A pitch class representation is provided by the chroma STFT, which depicts the spectral energy distribution of an audio signal in the chroma domain. The harmonic content of an audio stream is represented as a feature in machine learning. An audio signal's harmonic content can reveal information about the music's chord progression, melody, and tone. A machine learning model may be taught to categories an audio signal based on its harmonic content by extracting the Chroma STFT feature from the audio signal and feeding it as input into the model.

D. GRAPHICAL REPRESENTATION

A visual representation of frequency content of a signal in machine learning is spectrogram. The intensity of each frequency component in spectrographic representation is shown by a color and time is along the horizontal axis of graph. For generating a spectrogram, signals' domain is converted from time to frequency domain using Fourier transform. The resulting spectrum is then divided into smaller segments, and short-time Fourier transform is implicated to computing the frequency content of the signal. The intensity of respective component in the signal is represented by the color of the corresponding pixel. Spectrograms for Aluminum is shown in figure 5, while that of Mild Steel and Brass are shown in figures 6 and figure 7 respectively.

E. DATA FILES SEGREGATION AND FEATURES EXTRACTION

The data files are segregated based on their depth of cut, and class attributes are assigned to them, namely New, Used, and Worn-Out tools. Feature extraction is then carried out on each of these attributed data files in time-frequency domains. To facilitate the feature extraction process and training, the data is divided into seconds. The length of each class variable for Aluminum is 241, 249, and 230, respectively. The key features extracted are specialized for analyzing and manipulating acoustic data and have already been explained in detail above. The class attribute shown in table 3 below refers to tool conditions either as New, Used and Worn-out.

The sample data frame and respective class attributes of extracted features including Mel-frequency Cepstral Coefficients, Spectral Centroid, Root Mean Square Error, Spectral Bandwidth, Spectral Roll-off, Zero Crossing Rate, Spectral Contrast, and Chroma STFT are shown in table 3 below.

F. BUILDING LSTM MODEL

A calling function build_model is used for creating neural network model with a specified input shape for tasks based on time-series sequential data. Basically, our data comprise 08-time steps/features with a single dimension at each step. The model architecture is composed of different layers including LSTM, dense, drop-out with activation functions. The dataset is separated into two subdivisions: the training dataset and the test data. The training set trains the machine learning model, whereas the test set assess model's performance. In our case, test size $= 0.3$ i.e.: 30% of the dataset will be used for testing, while the remaining 70% will be used for training. The model will be validated by a random data set. We have created a callback in TensorFlow's Keras API for model checkpointing during the training step. Based on our monitoring protocol predefined, only the best model is saved and the model keep on getting replaced when new model with better validation performance is found during training. This method applies the same scaling transformation to the test data as was applied to the training data, using the mean and standard deviation computed during the training phase. By scaling the data using Standard Scaler object on

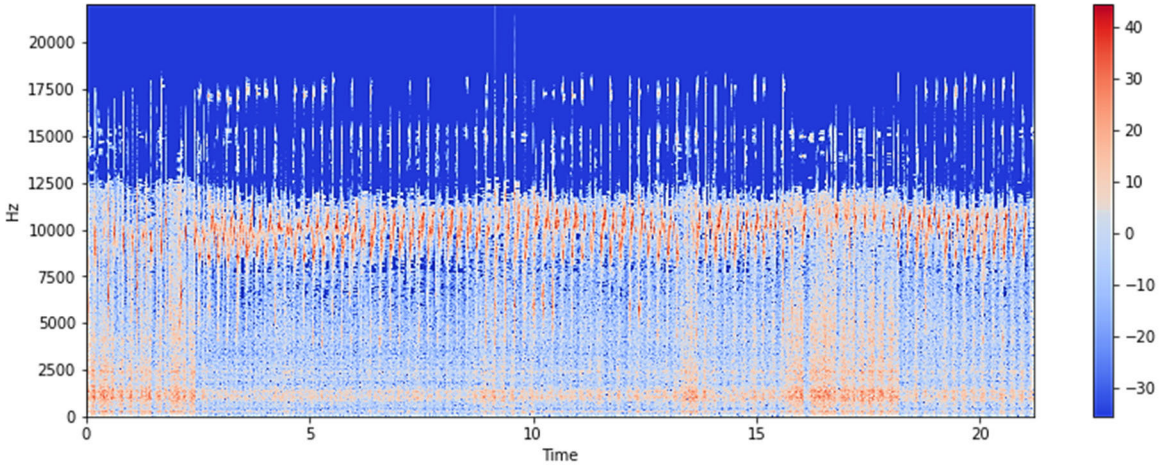

FIGURE 6. Spectrogram of mild steel.

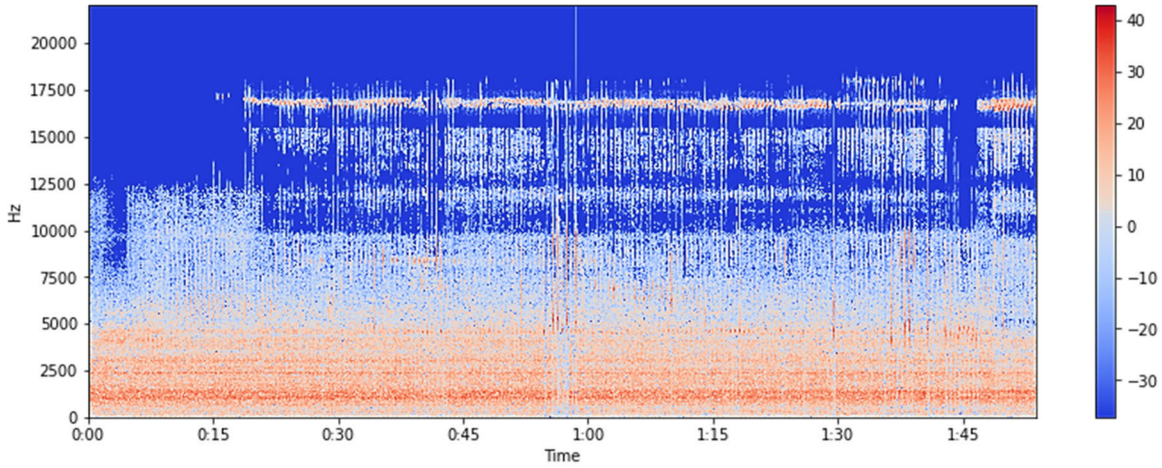

FIGURE 7. Spectrogram of brass.

both training and test data, we ensure that the two datasets are scaled consistently and can be compared and evaluated in a meaningful way.

G. LSTM MODEL PARAMETERS

While building LSTM model, a sequential model object was created in Keras framework. We have three classes of data for which a linear stack of layers is created. In this mode, 64 fully connected dense layers and LSTM memory cells are added to the sequential model object. To introduce non-linearity and the model to be able to handle more complex patterns, an activation function, Softmax is added to the model object. Dropout layers are also added as it is a regularization technique that helps prevent overfitting by randomly setting a fraction of the inputs to the layer to zero during training. This has the effect of ''dropping out'' some of the neurons in the layer and forcing the remaining neurons to learn more robust and generalizable features. The training process is conducted using multiple number of epochs which denotes a single pass of the entire training dataset through the model during training. The model will process the entire training dataset once during this epoch and update its parameters (weights and biases) based on the loss function and the optimizer used in the training process. The validation metrics can be used to decide whether to stop the training early or adjust the learning rate or other hyperparameters. The progress of the training process is monitored through call backs and model loss function. The value loss is continuously monitored and improved using call back function and accordingly weights, biases and hyperparameters are updated to get desired model training accuracy.

V. RESULTS AND DISCUSSION

The tool flank wear conditions are pre-defined when starting the experimental procedure. The three tool conditions were; New, Used and Worn-out. It was observed that, the resulting sound signals for new tools were having lower intensity as compared to used and worn-out ones. Additionally, the

TABLE 3. Class attributes of extracted features of aluminum, mild steel and brass.

S. #	mfcc	rmse	chroma_stft	spect_cent	spect_bw	roll_off	zcr	spect_cont	class
0	-4.9815	0.1353	0.4787	2579.0192	1876.8936	4451.8866	0.0957	17.5494	Used
1	-5.2686	0.1359	0.4556	2544.2980	1761.3718	4418.5586	0.0999	17.5327	Worn-out
2	-5.4054	0.1345	0.4670	2547.7543	1716.2900	4399.3482	0.1023	17.6162	Worn-out
3	-4.9762	0.1355	0.4801	2575.4048	1872.9988	4448.4110	0.0955	17.5798	Used
4	-5.0038	0.1354	0.4847	2556.4771	1858.0503	4427.9774	0.0947	17.5206	Used

S. #	mfcc	rmse	chroma_stft	spect_cent	spect_bw	roll_off	zcr	spect_cont	class
0	-4.9639	0.1358	0.4933	2431.7176	2005.5790	4193.6647	0.0826	18.1384	Good
1	-5.0937	0.1323	0.4971	2604.3828	1762.3432	4407.8217	0.1080	17.7636	Worn-out
2	-5.5283	0.1352	0.4967	2551.0598	2126.2693	4351.4123	0.0862	18.0636	Good
3	-5.5787	0.1338	0.5041	2862.2316	2404.2625	5142.8385	0.0960	17.8632	Good
4	-4.9668	0.1358	0.4908	2426.5540	1999.9920	4181.5786	0.0825	18.1282	Good

S. #	mfcc	rmse	chroma_stft	spect_cent	spect_bw	roll_off	zcr	spect_cont	class
0	-3.8347	0.1314	0.4871	2887.2449	2118.0904	4831.8744	0.1094	17.3547	Good
1	-4.6153	0.1318	0.5132	3166.9585	2555.9468	5594.0495	0.1095	17.5325	Good
2	-4.0821	0.1383	0.4809	2461.8679	2026.9899	4105.6973	0.0828	17.3065	Worn-out
3	-4.7643	0.1394	0.4693	2858.6987	2209.3289	4819.7394	0.1004	17.8942	Used
4	-4.8799	0.1390	0.4734	2801.0751	2133.6100	4734.3604	0.0997	17.9114	Used

S. #	mfcc	rmse	chroma_stft	spect_cent	spect_bw	roll_off	zcr	spect_cont	class
0	-8.4776	0.1096	0.3778	5240.6360	3007.8358	8394.6606	0.1902	17.8741	New
1	-8.9757	0.1073	0.3696	5396.6093	3024.2690	8567.6713	0.1986	17.8629	New
2	-6.0428	0.1227	0.4027	4486.3480	3099.2273	7826.2590	0.1765	17.7713	Used
3	-5.9715	0.1207	0.4220	4535.5130	3014.3458	7836.8952	0.1826	17.7981	Used
4	-3.8710	0.1313	0.3996	2492.1162	1966.1757	4151.3991	0.0926	18.8229	Used

S. #	mfcc	rmse	chroma_stft	spect_cent	spect_bw	roll_off	zcr	spect_cont	class
0	-12.858	0.1492	0.2264	7734.4711	2972.9893	9855.8380	0.3299	18.1271	Used
1	-12.373	0.1417	0.2384	7392.8611	3028.3859	9752.4568	0.3143	18.2345	Used
2	-5.4032	0.1180	0.4273	4758.0365	3368.5710	8656.2334	0.1787	17.5333	Worn-out
3	-6.0450	0.1205	0.3809	5947.1892	4046.8581	10689.5450	0.2448	18.2842	New
4	-12.303	0.1393	0.2487	7280.2501	3048.2352	9712.4582	0.3077	18.2481	Used

S. #	mfcc	rmse	chroma_stft	spect_cent	spect_bw	roll_off	zcr	spect_cont	class
0	-12.524	0.1576	0.2328	7832.8498	3048.7467	10080.1518	0.3475	18.1603	Used
1	-3.7761	0.1248	0.3539	3142.9259	2492.2329	5005.0653	0.1064	18.5494	Used
2	-9.3724	0.1236	0.3435	7137.9851	3453.2038	10476.2085	0.3061	18.0481	Worn-out
3	-10.504	0.1233	0.3176	7233.4307	3361.5759	10470.9217	0.3038	18.3756	Worn-out
4	-3.2270	0.1275	0.3883	3312.9642	2630.8997	5527.5467	0.1143	18.2064	Used

TABLE 3. *(Continued.)* Class attributes of extracted features of aluminum, mild steel and brass.

S. #	mfcc	rmse	chroma_stft	spect_cent	spect_bw	roll_off	zcr	spect_cont	class
0	-0.1721	0.1261	0.4892	4327.0006	3703.7964	9182.6391	0.1429	17.2406	Worn-out
1	-0.8002	0.1234	0.4939	4802.3768	3818.7641	9816.3084	0.1738	17.4509	Worn-out
2	-8.3399	0.0557	0.4452	3095.3429	2393.6389	5956.0098	0.1362	17.4859	Used
3	-8.0225	0.0581	0.4412	3058.8305	2376.5089	5897.2176	0.1332	17.5030	Used
4	-3.2124	0.1362	0.4106	3384.6908	2960.0250	6823.4564	0.1053	17.9652	New

S. #	mfcc	rmse	chroma_stft	spect_cent	spect_bw	roll_off	zcr	spect_cont	class
0	-4.3226	0.1357	0.4863	2762.0533	2085.1515	4827.2531	0.0988	17.2396	Used
1	-4.1359	0.1350	0.4657	2739.7803	1968.3506	4962.8568	0.1024	17.4427	New
2	-3.6987	0.1290	0.4574	3827.7329	3699.6486	6861.6161	0.1566	17.5434	Worn-out
3	-4.6384	0.1307	0.4575	4310.3388	3965.1389	8599.7785	0.2049	17.8591	Worn-out
4	-4.2802	0.1351	0.4766	2651.7388	1844.4886	4589.3684	0.1014	17.5081	New

S. #	mfcc	rmse	chroma_stft	spect_cent	spect_bw	roll_off	zcr	spect_cont	class
0	-3.9744	0.1334	0.4741	2641.8397	1760.8595	4540.8426	0.1062	17.2601	New
1	-4.1337	0.1345	0.4718	2720.6193	1935.5213	4768.5079	0.1027	17.5733	New
2	-3.5711	0.1340	0.5018	2774.3967	2155.2849	4929.4369	0.1015	17.2434	Worn-out
3	-3.2932	0.1354	0.5026	2644.5367	1990.9961	4664.3586	0.0947	17.1186	Worn-out
4	-3.7787	0.1334	0.4824	2508.6380	1642.8566	4332.8685	0.1031	17.1332	New

S. #	mfcc	rmse	chroma_stft	spect_cent	spect_bw	roll_off	zcr	spect_cont	class
0	-4.1663	0.1358	0.4667	2756.6599	2037.8572	4827.5936	0.1006	17.6008	New
1	-3.7959	0.1338	0.4761	2921.6117	2226.4919	4980.3981	0.1148	17.1705	Worn-out
2	-3.8502	0.1347	0.5017	2722.0948	1908.0439	4681.0037	0.1050	17.3884	New
3	-4.3186	0.1356	0.4742	2657.6700	2065.7463	4507.8906	0.0936	17.2412	Used
4	-3.9110	0.1343	0.4819	2508.7286	1837.0527	4372.7113	0.0929	17.2037	Used

S. #	mfcc	rmse	chroma_stft	spect_cent	spect_bw	roll_off	zcr	spect_cont	class
0	-3.6190	0.1350	0.4944	2630.0793	1842.2440	4522.4689	0.1002	17.1190	New
1	-3.4942	0.1376	0.4465	2690.3176	2186.7416	4583.7394	0.0917	17.6489	Used
2	-4.1296	0.1365	0.4693	2604.6099	2093.7150	4457.1379	0.0885	17.1640	Used
3	-4.3075	0.1367	0.4802	2687.2589	2008.7838	4723.5973	0.0955	17.4045	New
4	-2.4147	0.1337	0.4359	3829.5108	3396.7478	7442.6369	0.1531	17.2919	Worn-out

sound intensity was lower for first pass and kept increasing in subsequent passes with highest at maximum depth of cut. The worn-out tool produced highest intensity sound signals with maximum depth of cut. The LSTM model is trained using the pre-processed datasets of acoustic signals. There are several key components that contribute to the model's architecture and behavior during training. They are epochs, biases and weights which are trainable parameters of LSTM model. The model was initially trained using pre-processed Aluminum, Mild Steel and Brass dataset having multiple depths of cut as explicitly explained. The acquired audio datasets are converted to .wav format as it is lossless and high quality uncompressed compared to .mp3 audio datasets. The array of signals for all workpieces comprised two

TABLE 4. Model accuracy for aluminum workpiece.

ALUMINUM WORKPIECE				
S. #	**Depth of Cut**	**Training Accuracy**	**Validation Accuracy**	**Testing Accuracy**
1.	01 MM	1.000	0.9954	0.9953
2.	02 MM	0.9973	0.9875	0.9875
3.	03 MM	0.9975	0.9882	0.9881

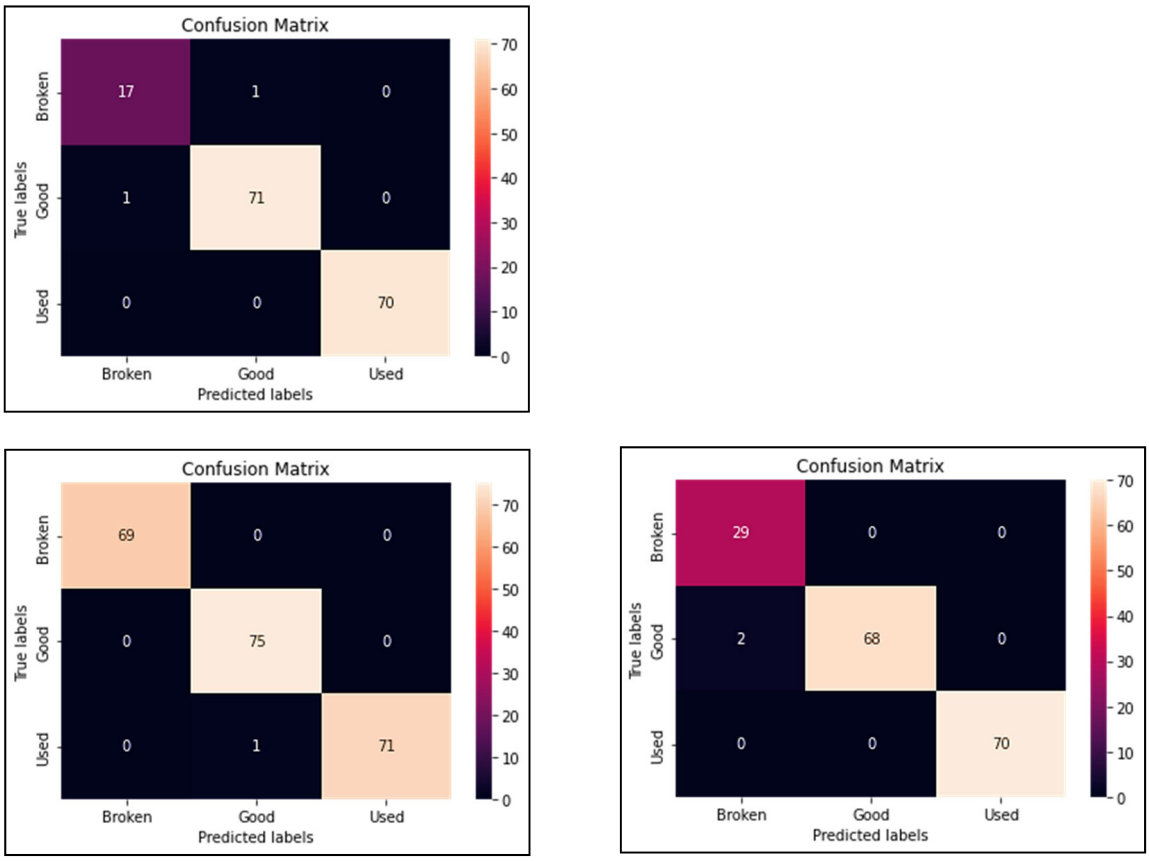

FIGURE 8. Confusion matrix of aluminum (1mm, 2mm, 3mm).

channels, indicating it's stereo. The meta dataset was formatted to Pandas DataFrame, preprocessed and their features were extracted using pandas libraries.

In proposed model, the model learning rate is 0.001. The model is trained through multiple epochs as specified explicitly for each workpiece with weights constantly been updated until the model is converged to get enhanced model performance and accuracy. The model is continuously evaluated using accuracy during its training till desired number of epochs are reached and multi-class model assessment is performed by the end.

A. ALUMINUM METRICS EVALUATION

The model training performance was assessed and found its accuracy as 0.9982. As the nodes weights were continuously updated through subsequent epochs, model accuracy was increased and a decrease in value loss was observed. The desired results/output for 01MM, 02MM and 03MM depths of cut was reached at 100th epoch where model training, validation & testing accuracies are shown in table 4. In LSTM (Long Short-Term Memory) models, loss and accuracy are two important metrics used for evaluating performance of the model. Model accuracy evaluate how well the model is able to classify the input correctly. Model loss indicates how well the model is able to predict the correct output for a given input. The accuracy is calculated by comparing the predicted output to the actual output and counting the number of correct predictions. For such comparison, one of the most typical methods is confusion matrix.

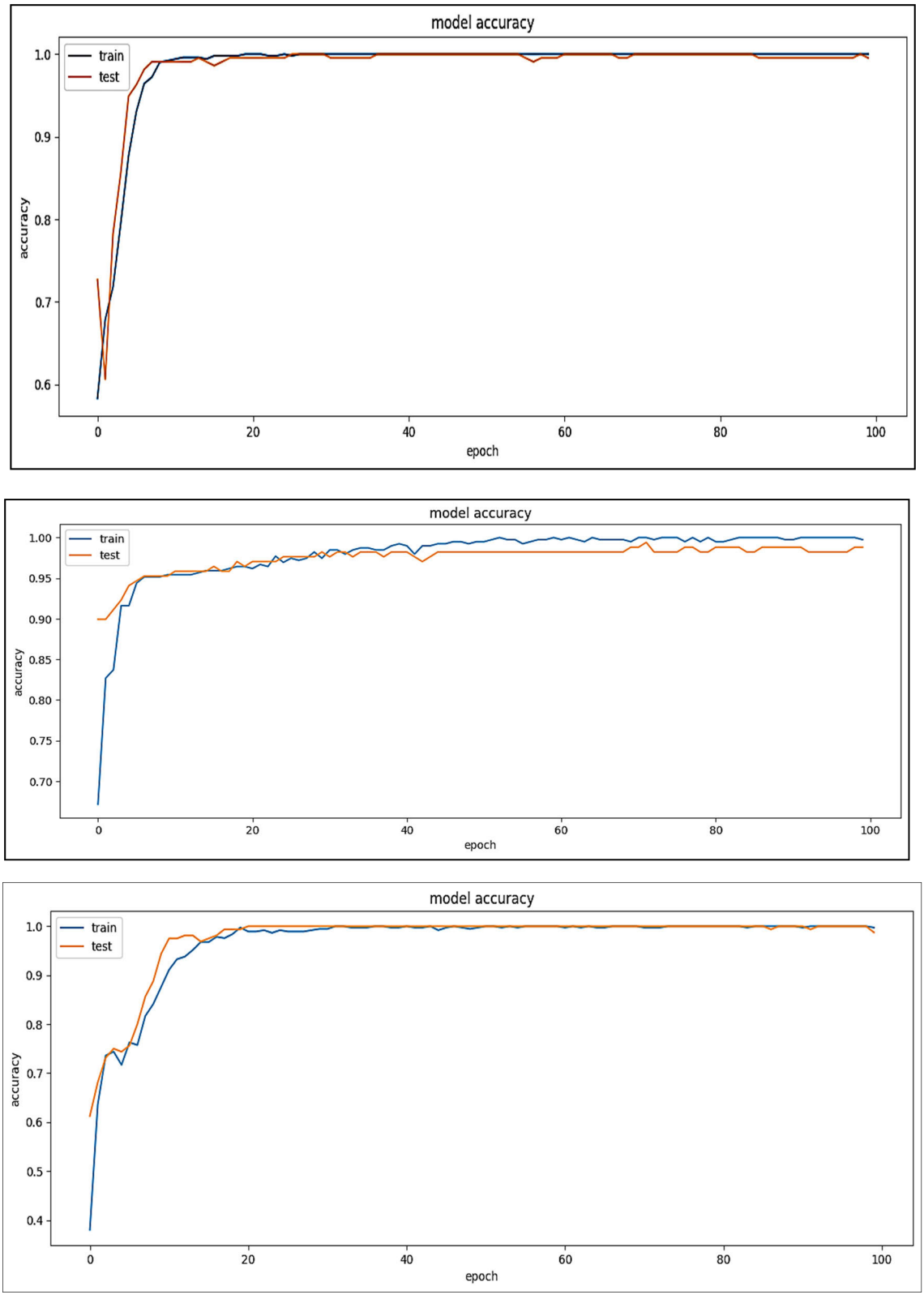

FIGURE 9. Model accuracy of aluminum (1mm, 2mm, 3mm).

1) MODEL ACCURACY

A confusion matrix is a graphical matrix used to appraise the performance of a machine learning model. It is a matrix that shows the ''number of true positives (TP), false positives (FP), true negatives (TN), and false negatives (FN)'' for a binary classification problem. In a confusion matrix, rows

TABLE 5. Model accuracy for mild steel workpiece.

MILD STEEL WORKPIECE				
S. #	**Depth of Cut**	**Training Accuracy**	**Validation Accuracy**	**Testing Accuracy**
1.	01 MM	1.000	0.9800	0.9800
2.	02 MM	0.9953	0.9784	0.9785
3.	03 MM	1.000	0.9545	0.9545
4.	04 MM	0.9962	0.9737	0.9737

represent the actual labels, while the columns represent the predicted class tags. Confusion matrix helps us in calculating several performance metrics like accuracy, precision, recall, and F1 score. The four possible outcomes are:

True Positives (TP): Correct and accurate prediction of a positive class.

False Positives (FP): Incorrect prediction of a positive class.

True Negatives (TN): Correct and accurate prediction of a negative class.

False Negatives (FN): Incorrect prediction of a negative class.

The underlying methodology followed for Aluminum, Mild Steel and Brass workpieces is same. The input signal is chopped into seconds contributing a total of 720 datapoints for Aluminum workpiece. Class attributes from new, used and worn-out are extracted from each datapoint of chopped datasets for training the LSTM model. To assess model performance, model accuracies are calculated. The data is divided into training and testing datasets with 70/30 ratio. During model building, learning rate, model optimizer and model loss functions are defined in sequential model. Appropriate dense, LSTM, and dropout layers are predefined as input to training model.

The fully connected dense layers defined the architecture comprising variable batch sizes as input with number of neurons and the dimensionality of each output represented as (None, 8, 64) having 128 parameters. The LSTM layer (None, 64) comprised variable batch size as input giving output with a dimensionality of 64 at each time step in the sequence processing over more than 33000 parameters. Similarly, the dropout layers and additional dense layers are introduced as per architectural criteria. The total trainable parameters in this scenario were 37,507, incorporated through multiple dense, LSTM and dropout layers. The model is trained till desired epochs are reached and model accuracy and losses are continuously monitored. Conclusively, the trained model is evaluated, through confusion matrix and the model accuracies for Aluminum metal as shown in figures 8 & figure 9 respectively. The predicted true class labels of 1mm depth of cut are 215 out of total 216 leading to model accuracy of 99.53%. For 2mm depth of cut, the true class labels are 158 out of total 160, giving 98.75% model accuracy. Similarly, for 3mm, the true and total labels are 167 and 169, giving model training accuracy of 98.81% calculated as follows. The model accuracies are also represented graphically as in figure 9.

$$\text{Model Accuracy} = \frac{(\text{TP} + \text{TN})}{(\text{TP} + \text{TN} + \text{FP} + \text{FN})}$$

$$\text{Model Accuracy} = \frac{(69 + 75 + 71)}{(69 + 75 + 71 + 1)} = 99.53\%$$

$$\text{Model Accuracy} = \frac{(17 + 71 + 70)}{(17 + 71 + 70 + 1 + 1)} = 98.75\%$$

$$\text{Model Accuracy} = \frac{(29 + 68 + 70)}{(29 + 68 + 70 + 2)} = 98.81\%$$

B. MILD STEEL METRICS EVALUATION

The model was initially trained using pre-processed mild-steel dataset having 1mm depth of cut. The model training performing was assessed and found its average accuracy as 0.9978. As the nodes weights were continuously updated through subsequent epochs, model accuracy was increased and a decrease in value loss was observed. The desired results/output was reached at 100th epoch where model training, validation and testing accuracies for 01MM, 02MM, 03MM and 04MM depths of cut respectively are given in table 5:

1) MODEL ACCURACY

The input signal is chopped into seconds and class attributes from new, used and worn-out are extracted from each datapoint. For assessing the model performance, model accuracies are calculated for which data is divided into training and testing datasets having 70% as training and 30% as testing dataset. As previously explained, during model building, learning rate, model optimizer and model loss functions are defined in sequential model. Here as well, the fully connected dense layers defined the architecture comprised variable batch sizes as input with number of neurons and the dimensionality of each output. The LSTM layer comprised variable batch size as input giving output with a dimensionality of 64 at each time step in the sequence processing over more than 54000 parameters. Similarly, the dropout layers and more dense layers are introduced as per architectural criteria. The total trainable parameters in this scenario were 54,019, incorporated through multiple dense, LSTM and dropout layers. After that, the model is trained till desired

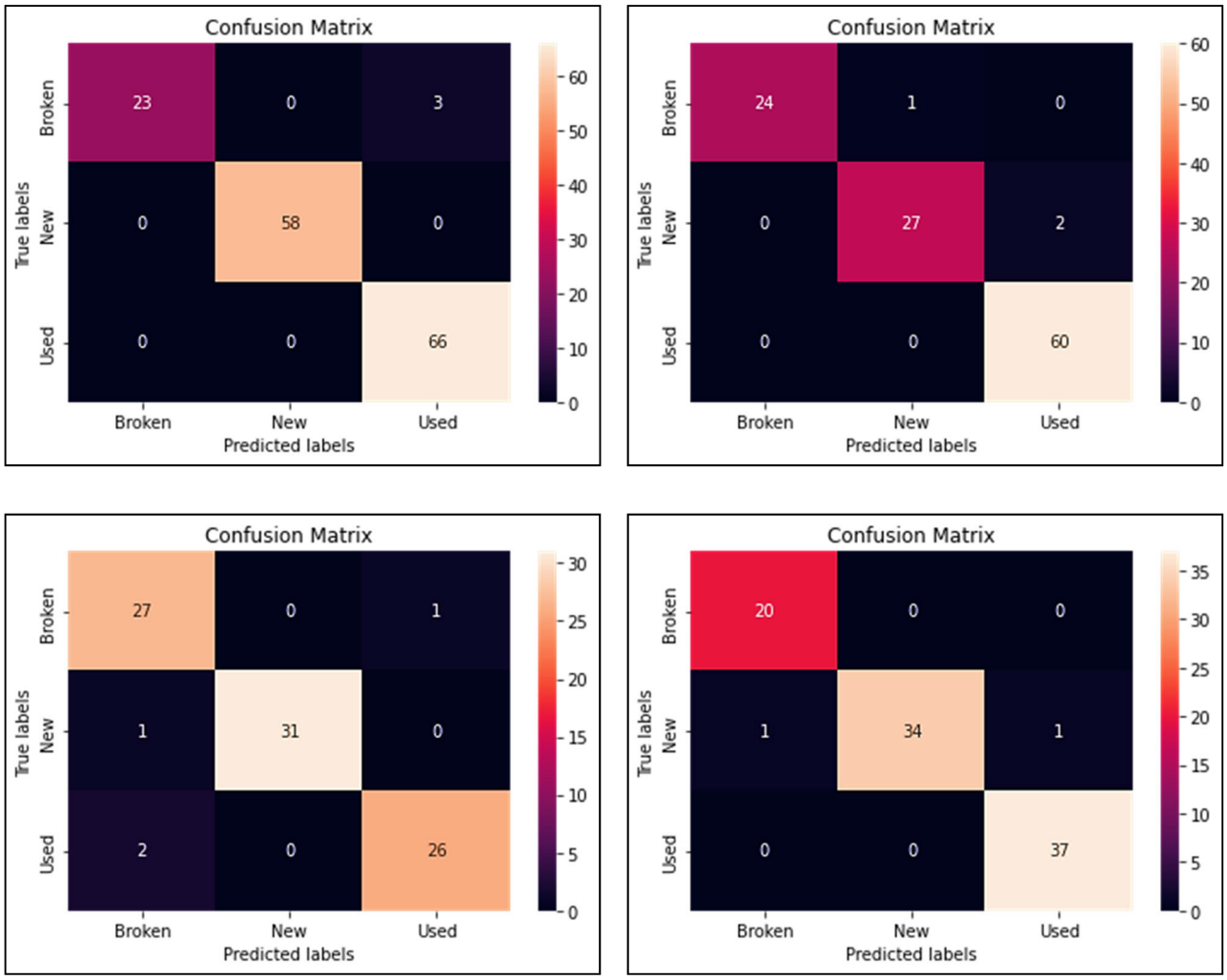

FIGURE 10. Confusion matrix of mild steel (1mm, 2mm, 3mm, 4mm).

epochs are reached and model accuracy and losses are continuously monitored. The trained model is evaluated, through confusion matrix and the model accuracies for Mild Steel metal as shown in figures 10 & figure 11 respectively. The predicted true class labels of 1mm depth of cut are 147 out of total 150 leading to model accuracy of 98.00%. For 2mm depth of cut, the true class labels are 91 out of total 93, giving 97.84% model accuracy. Similarly, for 3mm and 4mm, the true labels are 84 and 111, giving model training accuracy of 95.45% and 97.36% respectively.

In LSTM (Long Short-Term Memory) models, loss and accuracy are two important metrics used for evaluating performance of the model. The confusion matrix and the model accuracy for mild steel metal with depths of cut 1mm, 2mm, 3mm and 4mm are shown in figure 10 and figure 11 respectively. The model accuracy can also be calculated analytically as follows:

$$\text{Model Accuracy} = \frac{(\text{TP} + \text{TN})}{(\text{TP} + \text{TN} + \text{FP} + \text{FN})}$$

$$\text{Model Accuracy} = \frac{(23 + 58 + 66)}{(23 + 58 + 66 + 3)} = 98.00\%$$

$$\text{Model Accuracy} = \frac{(20 + 34 + 37)}{(20 + 34 + 37 + 1 + 1)} = 97.84\%$$

$$\text{Model Accuracy} = \frac{(27 + 31 + 26)}{(27 + 31 + 26 + 4)} = 95.45\%$$

$$\text{Model Accuracy} = \frac{(24 + 27 + 60)}{(24 + 27 + 60 + 2 + 1)} = 97.36\%$$

C. BRASS METRICS EVALUATION

The model was initially trained using pre-processed Brass dataset having 1mm depth of cut. The model training performing was accessed and found its accuracy as 0.9897. As the nodes weights were continuously updated through subsequent epochs, model accuracy was increased and a decrease in value loss was observed. The desired results for 01MM, 02MM, 03MM and 04MM depths of cut was reached at 100th epoch where training, validation & testing accuracies of model respectively are given as in table 6:

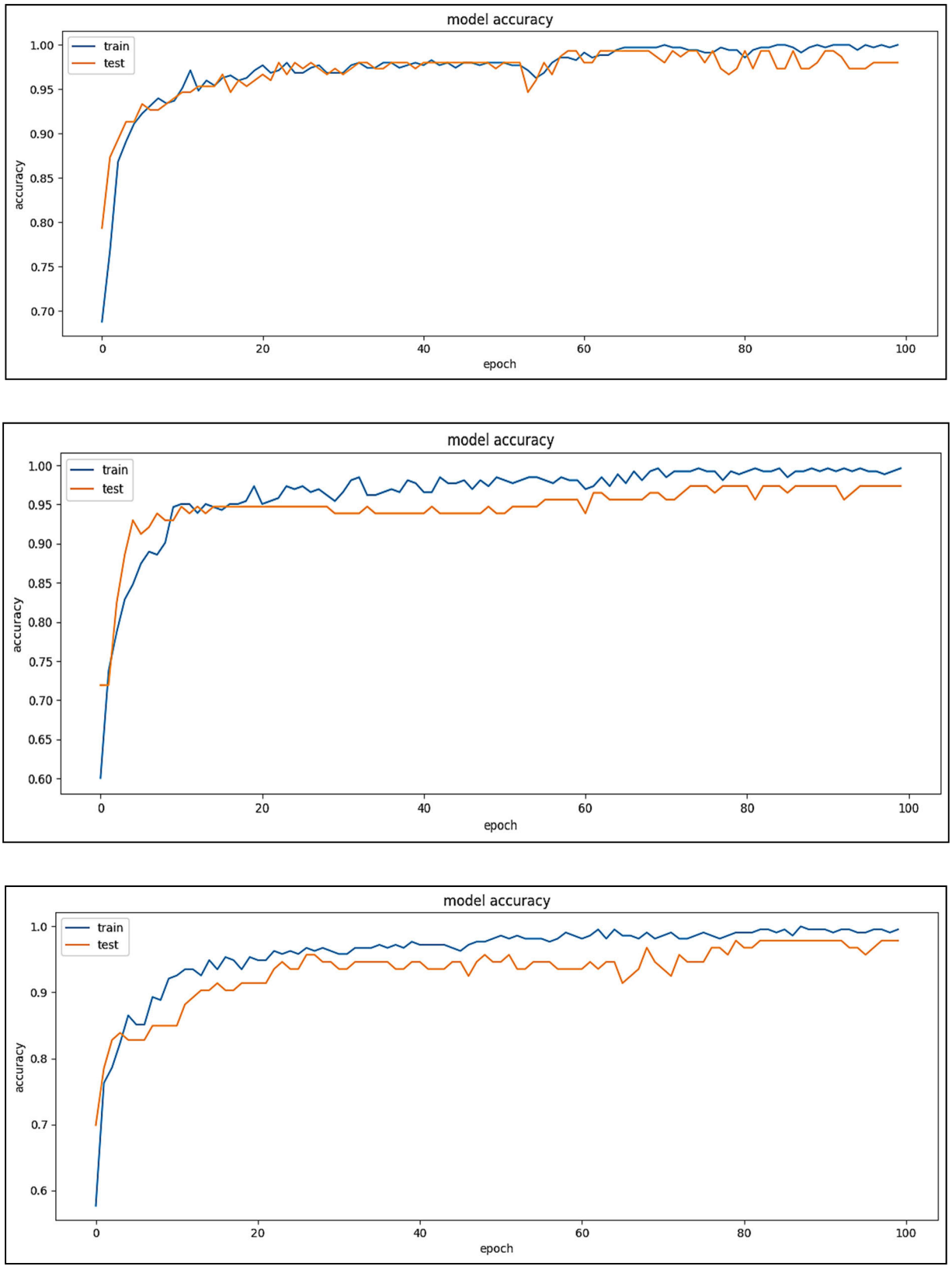

FIGURE 11. Model accuracy of mild steel (1mm, 2mm, 3mm, 4mm).

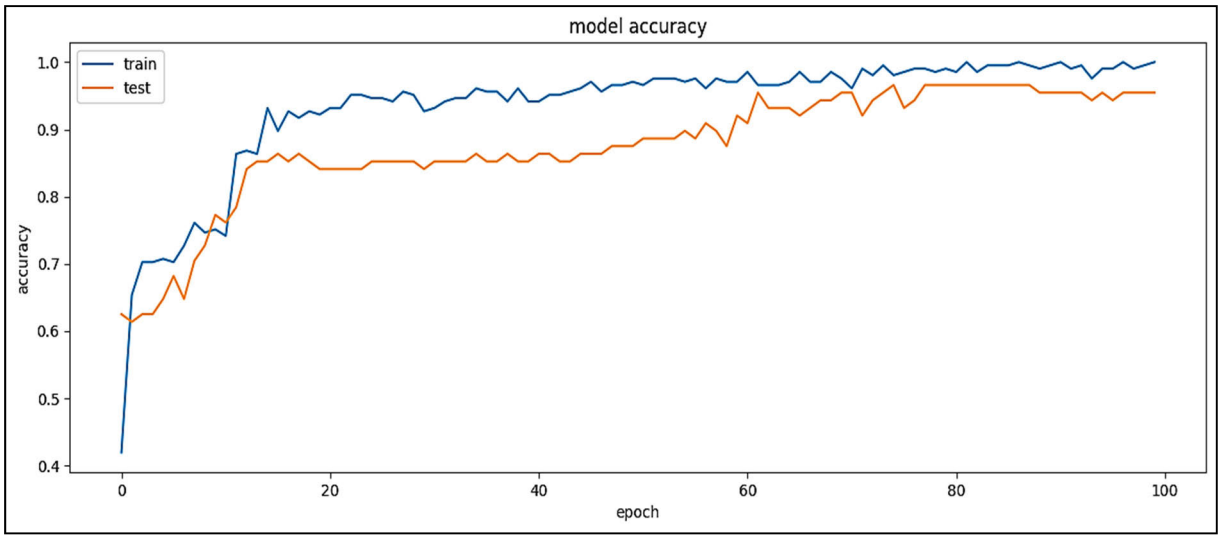

FIGURE 11. *(Continued.)* **Model accuracy of mild steel (1mm, 2mm, 3mm, 4mm).**

TABLE 6. Model accuracy for brass workpiece.

BRASS WORKPIECE				
S. #	**Depth of Cut**	**Training Accuracy**	**Validation Accuracy**	**Testing Accuracy**
1.	01 MM	0.9714	0.9464	0.9464
2.	02 MM	0.9922	0.9940	0.9939
3.	03 MM	1.000	1.000	0.9939
4.	04 MM	0.9955	0.9793	0.9792

1) MODEL ACCURACY

The input signal acquired during machining of Brass workpiece is chopped into seconds and respective class attributes are extracted from each datapoint. For assessing the model performance, model accuracies are calculated for which data is divided into training and testing datasets, 70%:30%. During model building, learning rate, model optimizer and model loss functions are defined in sequential model. The fully connected dense layers defined the architecture comprised variable batch sizes as input with multiple number of predefined neurons and the dimensionality of each output. The LSTM layer comprised variable batch size as input giving output with a dimensionality of 64 at each time step in the sequence processing over more than 37000 parameters. Similarly, the dropout layers and more dense layers are introduced as per architectural criteria. The total trainable parameters in this scenario were 37, 507, incorporated through multiple dense, LSTM and dropout layers. The model is trained till desired epochs are reached and model accuracy and losses are continuously monitored. The trained model is evaluated, through confusion matrix and the model accuracies for Brass metal as shown in figures 12 & figure 13 respectively. The predicted true class labels of 1mm depth of cut are 159 out of total 168 leading to model accuracy of 94.64%. For 2mm depth of cut, the true class labels are 165 out of total 166, giving 99.39% model accuracy. Similarly, for 3mm and 4mm, the true labels are 163 and 189 giving model training accuracies of 99.39% and 97.92% respectively.

In LSTM (Long Short-Term Memory) models, loss and accuracy are two important metrics used to evaluate the performance of the model. The confusion matrix and the model accuracy for Brass alloy with depths of cut 1mm, 2mm, 3mm and 4mm are respectively shown in figure 12 and figure 13 below.

$$\text{Model Accuracy} = \frac{(\text{TP} + \text{TN})}{(\text{TP} + \text{TN} + \text{FP} + \text{FN})}$$

$$\text{Model Accuracy} = \frac{(34 + 58 + 67)}{(34 + 58 + 67 + 9)} = 94.64\%$$

$$\text{Model Accuracy} = \frac{(36 + 66 + 63)}{(36 + 66 + 63 + 1)} = 99.39\%$$

$$\text{Model Accuracy} = \frac{(32 + 65 + 66)}{(32 + 65 + 66 + 1)} = 99.39\%$$

$$\text{Model Accuracy} = \frac{(62 + 63 + 64)}{(62 + 63 + 64 + 3 + 1)} = 97.92\%$$

VI. MULTICLASS MODEL ASSESSMENT

In a multi-class classification matrix, we use different model assessment metric for evaluating performance of model. They include: Confusion Matrix, Precision, Accuracy, Recall and

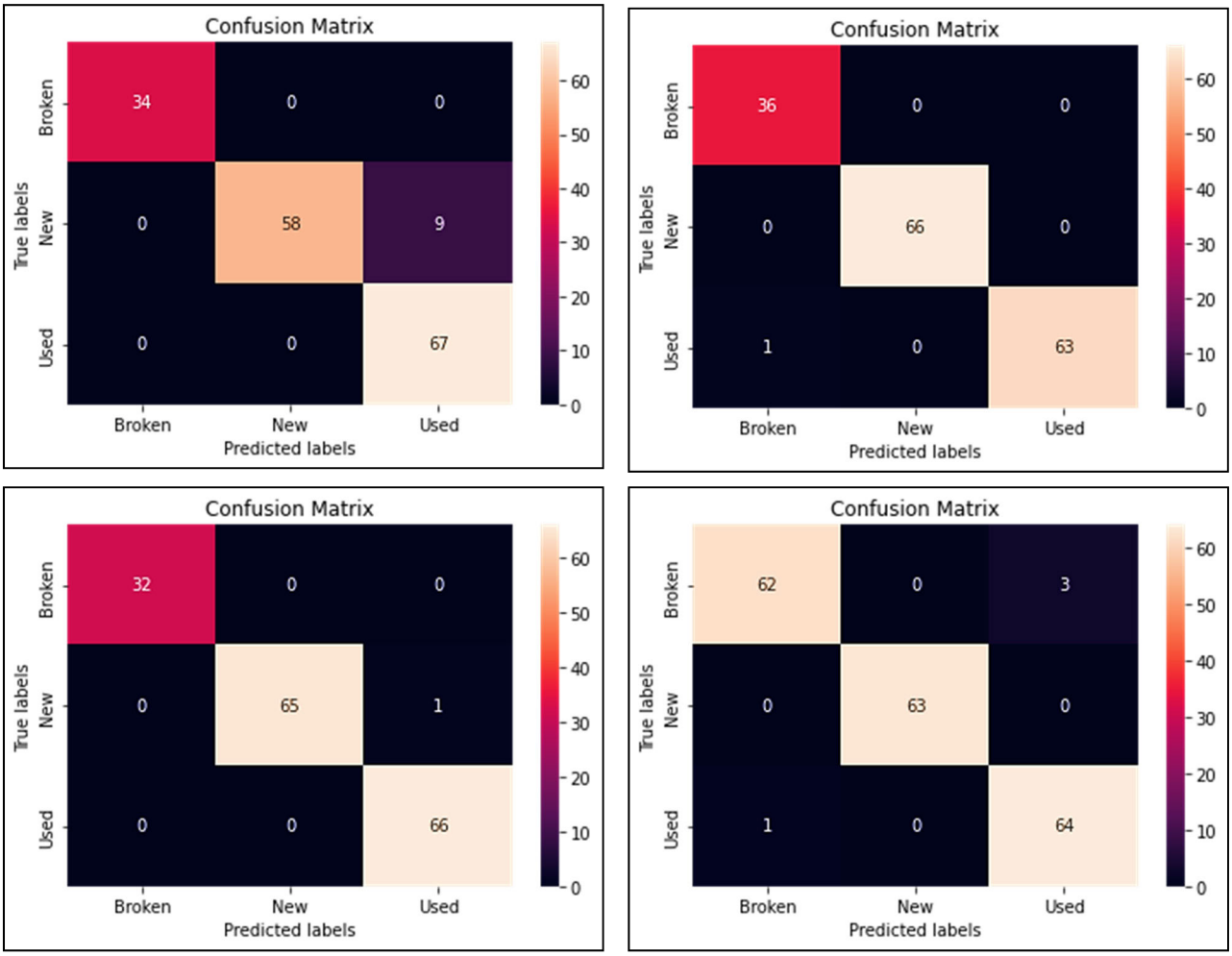

FIGURE 12. Confusion matrix of brass (1mm, 2mm, 3mm, 4mm).

F1-Score. Confusion matrix has already been elaborated in detail as above.

Precision of model defines the ratio of actual and correct outputs to total ones made by the trained model. Precision of each class is given in table 7 and shown mathematically as:

$$\text{Precision} = \text{Correctly Predicted/Total Predicted}$$

Recall of a model shows the proportion of number of TPs to total TPs and FNs as in table 8 and shown mathematically as:

$$\text{Recall} = \text{CorrectlyClassified/ActualTotal}$$

$$\text{Recall} = \text{CorrectlyClassified/ActualTotal}$$

F-score shown in table 10, means the weighted average of precision and recall and shown mathematically as:

$$\text{F} - \text{Score} = 2\text{X(RecallXPrecision)/(Recall} + \text{Precision)}$$

$$\text{F} - \text{Score} = 2\text{X(RecallXPrecision)/Recall} + \text{Precision}$$

A model with an an average F1-score of 97.50% is doing both precision and recall extremely well. It implies that the model is capable of accurately predicting positive outcomes and is effective at capturing the majority of actual positive situations. This F-1 Score would be highly regarded as good in many classification tasks, suggesting a highly successful model.

VII. CONCLUSION AND FUTURE WORK

In the machining industry, there has been a significant focus on research and development aimed at creating a tool health classification system. Traditionally, tool wear monitoring and classification have relied on human operators who visually inspect the tool and make judgments based on their expertise and experience. Unfortunately, this approach is subjective and can lead to mistakes, resulting in unnecessary tool replacements or machining failures. Providentially, with the advent of AI, the tool health monitoring and classification process has been revolutionized. Conventional AI systems employ rule-based models to analyze sensor data and determine the tool's health condition. However, these systems require relevant feature selection and sensor data preprocessing, which can be time-consuming and necessitate considerable domain knowledge. On the other hand, advanced AI techniques like machine learning (ML) have demonstrated great potential in enhancing the accuracy and efficiency of tool health classification. Long Short-Term Memory Networks is one of those advanced deep learning approaches being used in our scope our research.

Experimental procedure was conducted and the machine spindle's revolution per minute (RPM) and the workpiece's

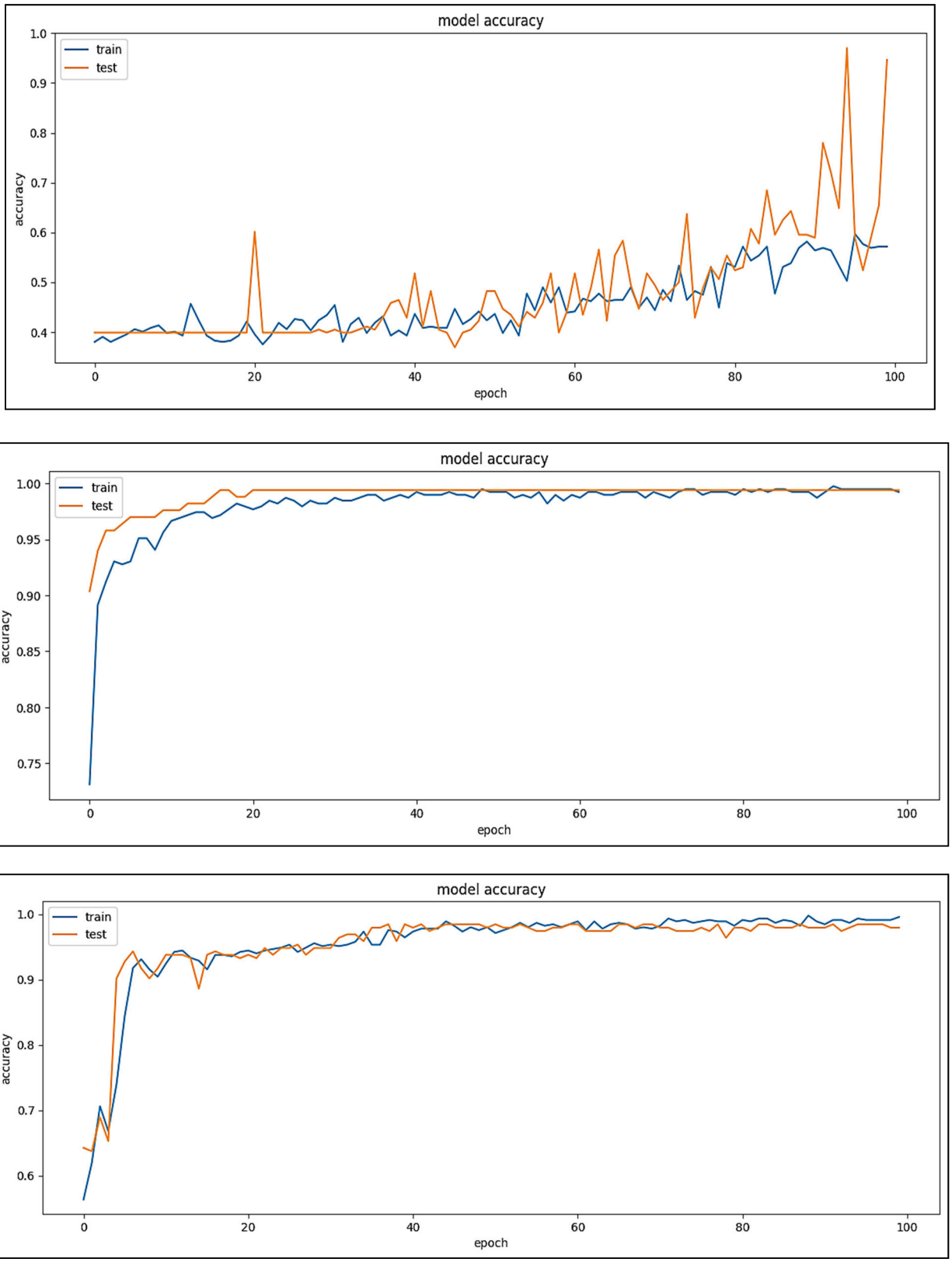

FIGURE 13. Model accuracy of brass (1mm, 2mm, 3mm, 4mm).

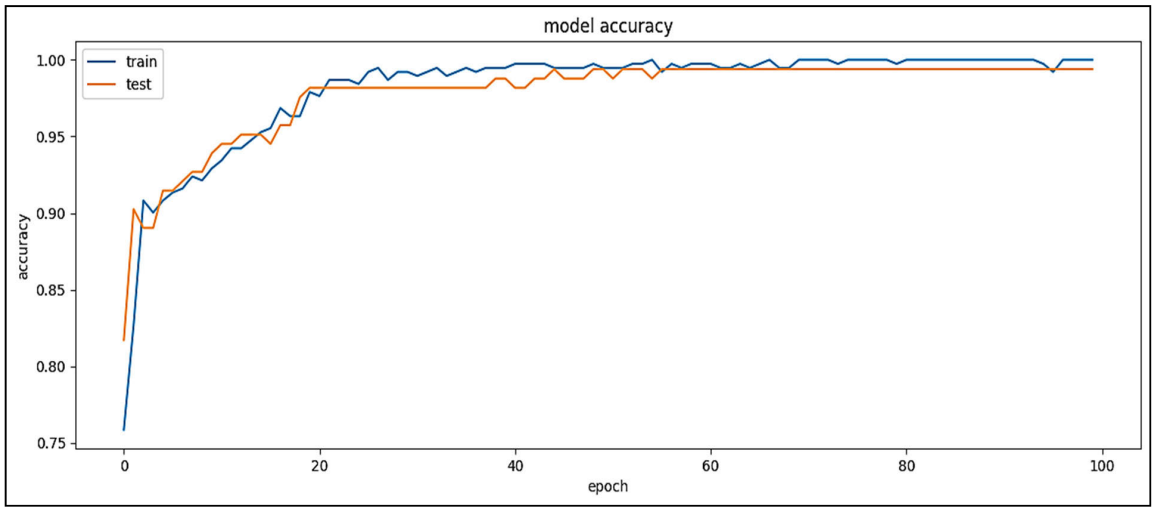

FIGURE 13. *(Continued.)* Model accuracy of brass (1mm, 2mm, 3mm, 4mm).

TABLE 7. Precision of model classes.

Class	Aluminum			Mild Steel				Brass			
	1 MM	2 MM	3 MM	1 MM	2 MM	3 MM	4 MM	1 MM	2 MM	3 MM	4 MM
New	0.9868	0.9861	1.00	1.00	0.9523	1.00	0.9643	1.00	1.00	1.00	1.00
Used	1.00	1.00	1.00	0.9565	0.9737	0.9629	0.9677	0.881	1.00	0.985	0.955
Worn-Out	1.00	0.9440	0.9350	1.00	0.9523	0.900	1.00	1.00	0.973	1.00	0.984

TABLE 8. Recall of model classes.

Class	Aluminum			Mild Steel				Brass			
	1 MM	2 MM	3 MM	1 MM	2 MM	3 MM	4 MM	1 MM	2 MM	3 MM	4 MM
New	1.0	0.9861	0.9714	1.00	0.9444	0.9687	0.9310	0.866	1.00	0.984	1.00
Used	0.9861	1.00	1.00	1.00	1.00	0.9285	1.00	1.00	0.984	1.00	0.985
Worn-Out	1.00	0.9440	1.00	0.8846	1.00	0.942	0.9600	1.00	1.00	1.00	0.958

TABLE 9. F-Score of model classes.

Class	Aluminum			Mild Steel				Brass			
	1 MM	2 MM	3 MM	1 MM	2 MM	3 MM	4 MM	1 MM	2 MM	3 MM	4 MM
New	0.9936	0.9861	0.985	0.938	0.971	0.984	0.947	0.928	0.928	0.985	1.00
Used	0.9931	1.00	1.00	0.977	0.986	0.944	0.984	0.937	0.992	0.992	0.969
Worn-Out	1.00	0.944	0.966	1.00	0.975	0.931	0.979	1.00	0.941	1.00	0.971

TABLE 10. Average f-score of model classes.

Class	Aluminum	Mild Steel	Brass
	Average F-Score		
New	0.9882	0.9600	0.9602
Used	0.9977	0.9727	0.9725
Worn-Out	0.9700	0.9712	0.9780
Individual Average	**0.9853**	**0.9680**	**0.9702**
Overall Average	**0.9750**		

feed rate were maintained at a constant 450 RPM and 0.5 mm/sec, respectively. The variable in the experiment was the depth of cut (DOC), ranging from 1 MM to 4 MM across different cases. We utilized three types of workpieces for our experiment: Mild Steel (MS), Brass, and Aluminum. The cutting tool used was made of HSS and had a fixed diameter of 10mm. To record the data, we employed three different tool conditions: New, Used, and Worn-out. The acoustic signals were acquired using a simple microphone.

The LSTM model was developed and underwent training, validation, and testing with various cutting depths and tool conditions, including new, used, and worn-out tools. The model's accuracy and test loss were evaluated, and the results were promising, achieving a testing accuracy of over 98%. Ultimately, the model showed the capability to accurately predict the tool state for a randomly selected dataset, consisting of various types of workpieces and tools. This way, our proposed LSTM model proved to be effective in tool state monitoring and demonstrated its capability to handle diverse tool conditions, making it a potentially valuable tool in the manufacturing industry.

Overall, the analysis demonstrated the efficacy of the model and its ability to accurately predict the output for various workpiece materials. This information could be valuable in the manufacturing industry, where the accurate prediction of output is crucial for ensuring the quality and efficiency of the production process.

We performed complete experimental and analytical procedures by keeping in due consideration the following 05 key factors:

No coolant was used during complete machining process.
Tool was fixed in chuck keeping fixed torque of 90 N.m.
Workpiece was fixed in vice with torque of 140 N.m.
Surrounding noise level was kept at minimal possible level.
Machine's sound & vibration was neglected.

In terms of future work, it is recommended to utilize a fixed flow rate of coolant throughout the entire experimental procedure. Additionally, modifying the fixed torque and collecting various datasets for analysis could also prove beneficial. Furthermore, a combination of two or more of the aforementioned conditions could be explored to generate an entirely new dataset and analytical procedure.

FUNDING

This work was supported by Researchers Supporting Project number (RSP2023R274), King Saud University, Riyadh, Saudi Arabia.

ACKNOWLEDGMENT

This work was supported by Researchers Supporting Project number (RSP2023R274), King Saud University, Riyadh, Saudi Arabia.

REFERENCES

[1] M. Arslan, K. Kamal, M. Fahad, S. Mathavan, and M. A. Khan, "Automated machine tool prognostics for turning operation using acoustic emission and learning vector quantization," in *Proc. 5th Int. Conf. Control, Autom. Robot. (ICCAR)*, Apr. 2019, pp. 468–472, doi: 10.1109/ICCAR.2019.8813739.

[2] T. Zafar, K. Kamal, Z. Sheikh, S. Mathavan, A. Jehanghir, and U. Ali, "Tool health monitoring for wood milling process using airborne acoustic emission," in *Proc. IEEE Int. Conf. Autom. Sci. Eng. (CASE)*, Aug. 2015, pp. 1521–1526, doi: 10.1109/CoASE.2015.7294315.

[3] M. Arslan, K. Kamal, M. F. Sheikh, M. A. Khan, T. A. H. Ratlamwala, G. Hussain, and M. Alkahtani, "Tool health monitoring using airborne acoustic emission and convolutional neural networks: A deep learning approach," *Appl. Sci.*, vol. 11, no. 6, p. 2734, Mar. 2021, doi: 10.3390/app11062734.

[4] K. Patra. *Acoustic Emission based Tool Condition Monitoring System in Drilling*. Accessed: Apr. 3, 2023. [Online]. Available: https://www.semanticscholar.org/paper/Acoustic-Emission-based-Tool-Condition-Monitoring-Patra/b295ccd97863c2cdfa1a5e2fa3378c4f58f37aa6

[5] T. Zafar, K. Kamal, R. Kumar, Z. Sheikh, S. Mathavan, and U. Ali, "Tool health monitoring using airborne acoustic emission and a PSO-optimized neural network," in *Proc. IEEE 2nd Int. Conf. Cybern. (CYBCONF)*, Jun. 2015, pp. 271–276, doi: 10.1109/CYBConf.2015.7175945.

[6] P. B. Huang, C.-C. Ma, and C.-H. Kuo, "A PNN self-learning tool breakage detection system in end milling operations," *Appl. Soft Comput.*, vol. 37, pp. 114–124, Dec. 2015, doi: 10.1016/j.asoc.2015.08.019.

[7] R. Koike, K. Ohnishi, and T. Aoyama, "A sensorless approach for tool fracture detection in milling by integrating multi-axial servo information," *CIRP Ann.*, vol. 65, no. 1, pp. 385–388, 2016, doi: 10.1016/j.cirp.2016.04.101.

[8] J. Sheikh-Ahmad, "Measurement of tool wear and dulling in the machining of particleboard," in *Proc. 13th Int. Wood Machining Seminar*, Jun. 1997, pp. 1–12, doi: 10.13140/2.1.4579.8086.

[9] C. Liu and L. Zhu, "A two-stage approach for predicting the remaining useful life of tools using bidirectional long short-term memory," *Measurement*, vol. 164, Nov. 2020, Art. no. 108029, doi: 10.1016/j.measurement.2020.108029.

[10] M. Marani, M. Zeinali, V. Songmene, and C. K. Mechefske, "Tool wear prediction in high-speed turning of a steel alloy using long short-term memory modelling," *Measurement*, vol. 177, Jun. 2021, Art. no. 109329, doi: 10.1016/j.measurement.2021.109329.

[11] B. Y. Lee, "Application of the discrete wavelet transform to the monitoring of tool failure in end milling using the spindle motor current," *Int. J. Adv. Manuf. Technol.*, vol. 15, no. 4, pp. 238–243, Apr. 1999, doi: 10.1007/s001700050062.

[12] A. Rastegari, A. Archenti, and M. Mobin, "Condition based maintenance of machine tools: Vibration monitoring of spindle units," in *Proc. Annu. Rel. Maintainability Symp. (RAMS)*, Jan. 2017, pp. 1–6, doi: 10.1109/RAM.2017.7889683.

[13] P. Y. Sevilla-Camacho, J. B. Robles-Ocampo, J. C. Jauregui-Correa, and D. Jimenez-Villalobos, "FPGA-based reconfigurable system for tool condition monitoring in high-speed machining process," *Measurement*, vol. 64, pp. 81–88, Mar. 2015, doi: 10.1016/j.measurement.2014.12.037.

[14] D. R. Salgado, F. J. Alonso, I. Cambero, and A. Marcelo, "In-process surface roughness prediction system using cutting vibrations in turning," *Int. J. Adv. Manuf. Technol.*, vol. 43, nos. 1–2, pp. 40–51, Jul. 2009, doi: 10.1007/s00170-008-1698-8.

[15] C. Gao, W. Xue, Y. Ren, and Y. Zhou, "Numerical control machine tool fault diagnosis using hybrid stationary subspace analysis and least squares support vector machine with a single sensor," *Appl. Sci.*, vol. 7, no. 4, p. 346, Mar. 2017, doi: 10.3390/app7040346.

[16] K. Szwajka and J. Górski, "Evaluation tool condition of milling wood on the basis of vibration signal," *J. Phys., Conf. Ser.*, vol. 48, pp. 1205–1209, Oct. 2006, doi: 10.1088/1742-6596/48/1/225.

[17] I. Yesilyurt and H. Ozturk, "Tool condition monitoring in milling using vibration analysis," *Int. J. Prod. Res.*, vol. 45, no. 4, pp. 1013–1028, Feb. 2007, doi: 10.1080/00207540600677781.

[18] J. K. Abbass and A. Al-Habaibeh, "A comparative study of using spindle motor power and eddy current for the detection of tool conditions in milling processes," in *Proc. IEEE 13th Int. Conf. Ind. Informat. (INDIN)*, Jul. 2015, pp. 766–770, doi: 10.1109/INDIN.2015.7281833.

[19] K. Harris, K. Triantafyllopoulos, E. Stillman, and T. McLeay, "A multivariate control chart for autocorrelated tool wear processes," *Qual. Rel. Eng. Int.*, vol. 32, no. 6, pp. 2093–2106, Oct. 2016, doi: 10.1002/qre.2032.

[20] D. R. Salgado and F. J. Alonso, "An approach based on current and sound signals for in-process tool wear monitoring," *Int. J. Mach. Tools Manuf.*, vol. 47, no. 14, pp. 2140–2152, Nov. 2007, doi: 10.1016/j.ijmachtools.2007.04.013.

[21] Q. Ren, S. Achiche, K. Jemielniak, and P. Bigras, "An enhanced adaptive neural fuzzy tool condition monitoring for turning process," in *Proc. IEEE Int. Conf. Fuzzy Syst. (FUZZ-IEEE)*, Jul. 2016, pp. 1976–1982, doi: 10.1109/FUZZ-IEEE.2016.7737934.

[22] N. Ghosh, Y. B. Ravi, A. Patra, S. Mukhopadhyay, S. Paul, A. R. Mohanty, and A. B. Chattopadhyay, "Estimation of tool wear during CNC milling using neural network-based sensor fusion," *Mech. Syst. Signal Process.*, vol. 21, no. 1, pp. 466–479, Jan. 2007.

[23] J. C. Jáuregui, J. R. Reséndiz, S. Thenozhi, T. Szalay, A. Jacsó, and M. Takács, "Frequency and time-frequency analysis of cutting force and vibration signals for tool condition monitoring," *IEEE Access*, vol. 6, pp. 6400–6410, 2018, doi: 10.1109/ACCESS.2018.2797003.

[24] X. Li, H.-X. Li, X.-P. Guan, and R. Du, "Fuzzy estimation of feed-cutting force from current measurement—A case study on intelligent tool wear condition monitoring," *IEEE Trans. Syst., Man Cybern. C, Appl. Rev.*, vol. 34, no. 4, pp. 506–512, Nov. 2004, doi: 10.1109/TSMCC.2004.829296.

[25] Y. Zhou and W. Xue, "Review of tool condition monitoring methods in milling processes," *Int. J. Adv. Manuf. Technol.*, vol. 96, nos. 5–8, pp. 2509–2523, May 2018, doi: 10.1007/s00170-018-1768-5.

[26] S. Kalyani and K. S. Swarup, "Study of neural network models for security assessment in power systems," *Int. J. Res. Rev. Appl. Sci.*, vol. 1, pp. 1–14, Nov. 2009.

[27] H. Rafezi, J. Akbari, and M. Behzad, "Tool condition monitoring based on sound and vibration analysis and wavelet packet decomposition," in *Proc. 8th Int. Symp. Mechatronics Appl.*, Apr. 2012, pp. 1–4, doi: 10.1109/ISMA.2012.6215170.

[28] C. K. Madhusudana, H. Kumar, and S. Narendranath, "Condition monitoring of face milling tool using K-star algorithm and histogram features of vibration signal," *Eng. Sci. Technol., Int. J.*, vol. 19, no. 3, pp. 1543–1551, Sep. 2016, doi: 10.1016/j.jestch.2016.05.009.

[29] R. H. L. da Silva, M. B. da Silva, and A. Hassui, "A probabilistic neural network applied in monitoring tool wear in the end milling operation via acoustic emission and cutting power signals," *Machining Sci. Technol.*, vol. 20, no. 3, pp. 386–405, Jul. 2016, doi: 10.1080/10910344.2016.1191026.

[30] S. Rangwala and D. Dornfeld, "Sensor integration using neural networks for intelligent tool condition monitoring," *J. Eng. Ind.*, vol. 112, no. 3, pp. 219–228, Aug. 1990, doi: 10.1115/1.2899578.

[31] J. Yu, S. Liang, D. Tang, and H. Liu, "A weighted hidden Markov model approach for continuous-state tool wear monitoring and tool life prediction," *Int. J. Adv. Manuf. Technol.*, vol. 91, nos. 1–4, pp. 201–211, Jul. 2017, doi: 10.1007/s00170-016-9711-0.

[32] W. Cai, W. Zhang, X. Hu, and Y. Liu, "A hybrid information model based on long short-term memory network for tool condition monitoring," *J. Intell. Manuf.*, vol. 31, no. 6, pp. 1497–1510, Aug. 2020, doi: 10.1007/s10845-019-01526-4.

FAWAD KHAN received the B.S. degree in mechanical engineering from the Ghulam Ishaq Khan Institute of Engineering Sciences and Technology (GIK), Khyber Pakhtunkhwa, in 2017, and the M.S. degree in mechanical engineering from the National University of Sciences and Technology (NUST), Islamabad. He is also working as the Deputy Manager and a Lead Maintenance Engineer with Pakistan Security Printing Corporation, Karachi.

KHURRAM KAMAL was born in Karachi, Pakistan. He received the B.E. degree in mechanical engineering from the NED University of Engineering and Technology, Karachi, in 2001, the master's degree in computer science from the University of Karachi, Karachi, in 2003, and the Ph.D. degree in mechatronics from Loughborough University, Loughborough, U.K., in 2008. Before the Ph.D. research, he was an Assistant Manager of production planning and control with the Press Shop Department, Pakistan Suzuki Motor Company Ltd., from 2003 to 2004. He is currently a Professor with the Department of Engineering Sciences, National University of Sciences and Technology, Islamabad, Pakistan. His research interests include artificial intelligence, image processing, embedded systems, intelligent machines, and condition-based maintenance.

TAHIR ABDUL HUSSAIN RATLAMWALA received the Ph.D. degree from Ontario Tech University, Canada. He is currently an Associate Professor with the National University of Sciences and Technology. His research interests include renewable hydrogen, renewable energy, sustainability, and AI in energy.

MOHAMMED ALKAHTANI received the B.Sc. degree in industrial engineering from King Saud University (KSU), Riyadh, Saudi Arabia, the M.Sc. degree in industrial engineering from the University of Central Florida, Orlando, FL, USA, and the Ph.D. degree in manufacturing engineering from Loughborough University, Loughborough, U.K. He was the Chairperson of the Industrial Engineering Department, College of Engineering, KSU, for over four years, from 2014 to 2018. He is currently a Professor of industrial engineering with the Industrial Engineering Department and the Vice Dean of the Advanced Manufacturing Institute, KSU. He has diverse expertise in analysis, modeling, and design of manufacturing systems, supply chain and operations management, responsiveness measurement, and leanness and agility in manufacturing and supply chain.

MOHAMMED ALMATANI received the M.Sc. and Ph.D. degrees in reliability and maintenance engineering from The University of Manchester. He is currently an experienced Faculty Member with King Saud University with a demonstrated history of working in the higher education industry. He is skilled in reliability modeling, industrial risk analysis, business process improvement, and lean asset management.

SENTHAN MATHAVAN (Member, IEEE) was born in Jaffna, Sri Lanka. He received the B.Sc. degree in mechanical engineering from the University of Peradeniya, Peradeniya, Sri Lanka, in 2005, and the Ph.D. degree in mechatronics from Loughborough University, Loughborough, U.K., in 2009. From 2005 to 2006, he was an Assistant Lecturer with the Mechanical Engineering Department, University of Peradeniya. From 2010 to 2011, he held a Rolls-Royce-funded postdoctoral research position with Loughborough University. He was a Mechatronics Engineer with ASML, The Netherlands, for five years. He was a Systems Architect with Nobleo Technology, The Netherlands, and is currently a Principal Mechanical Engineer with Cambridge Consultant, U.K. Since 2012, he has been a Visiting Fellow with Nottingham Trent University, Nottingham, U.K. He has carried out research and development in the aerospace, semiconductor, and transportation industries. His research interests include mechatronics, machine vision, and applied artificial intelligence.